CHARACTERIZATION OF AN OPTIMIZED HIGH PERFORMANCE CONCRETE WITH PARTIAL REPLACEMENT OF CEMENT BY FLY ASH AND NANOSILICA

By

Hildélix L. Soto Toro

A thesis submitted in partial fulfillment of the requirements for the degree of

MASTER OF SCIENCE
IN
CIVIL ENGINEERING

UNIVERSITY OF PUERTO RICO
MAYAGÜEZ CAMPUS
2018

Approved by:

Oscar Marcelo Suárez, Ph.D. President, Graduate Committee	Date
Felipe J. Acosta Costa, Ph.D. Member, Graduate Committee	Date
Arsenio Cáceres, Ph.D. Member, Graduate Committee	Date
Basir Shafiq, Ph.D. Member, Graduate Committee	Date
José Vega, Ph.D. Representative of Graduate Studies	Date
Ismael Págan Trinidad, MSC. Department Director	Date

ABSTRACT

Modern construction industry requires new technologies to comply with increasingly stricter environmental regulations. In particular, cutting back cement demand in concrete fabrication lowers carbon dioxide emissions caused by its production. One solution is cement replacement by other materials with smaller carbon footprints and equivalent cementitious properties, such as fly ash. This industrial waste material in contact with water turns into a cement-like paste. Alas, due to a slower reaction, at early age fly ash decreases the rate of strength gain in concrete. Counteracting such strength loss at early age with the addition of nanostructured silica motivated the present research. Furthermore, since the study of concrete mix with Portland cement, nanosilica, and fly ash can be complex and time-demanding, a statistical design of experiment for mixtures was developed. In this controlled experimental design, the compressive strength was response variable; the levels of Portland cement, fly ash and nanosilica were the independent factors whereas the water-to-binder ratio was kept constant. Five combinations of cement components were prepared for this design. Compressive, flexural and tensile strength results were measured at 7, 28 and 90 days of curing. On mixes with a 3% replacement with nanosilica, a strength development of 82% (of final resistance normalized at 90 days) was attained at 7 days. In addition, a 40% increment of compressive strength and a faster development of such strength were obtained by replacing part of cement with fly ash and nanosilica compared with mixtures containing only fly ash. Absorption and permeability test were conducted to identify properties which can eventually have an effect on concrete durability and other mechanical properties. This thesis reveals that a higher reduction of permeable voids and absorption is feasible in mixes with higher content of fly ash and nanoparticles. Finally, an analysis of the high performance concrete market, costs and concrete performance was used to evaluate costs of the product to, in the near future, develop a commercialization strategy.

RESUMEN

La industria de la construcción moderna requiere nuevas tecnologías para cumplir con las regulaciones ambientales cada vez más estrictas. En particular, la reducción de la demanda de cemento en la fabricación de hormigón reduce las emisiones de dióxido de carbono causadas por su producción. Una solución es el reemplazo de cemento por otros materiales con menos contaminantes y con propiedades cementicias equivalentes, como la ceniza volante. La ceniza volante es un bio-producto de la industria eléctrica que en contacto con el agua se convierte en una pasta similar al cemento. Por desgracia, debido a una reacción lenta, a temprana edad, las cenizas volantes disminuyen la razón de desarrollo de propiedades mecánicas en el hormigón. Este efecto provocado por el reemplazo de cenizas volantes en el hormigón motivó la presente investigación a incorporar sílice nanoestructurada para contrarrestar el desarrollo de resistencia tardío a temprana edad . Ha sido probado que la sílice activa el efecto puzzolánico en el hormigón. Dado que el estudio de la mezcla de concreto con cemento Portland, nanosílice y ceniza volante puede ser complejo y requerir mucho tiempo, se desarrolló un diseño estadístico de experimento para mezclas (DOE). Este diseño experimental se desarrolló con la resistencia a la compresión como variable de respuesta, y los niveles de cemento Portland, cenizas volantes y nanosílice, como factores independientes, mientras que la relación agua-cemento se mantuvo constante a 0.3. Se prepararon cinco combinaciones de componentes cementicios para este diseño. Los resultados de compresión, flexión y resistencia a la tracción se midieron a los 7, 28 y 90 días de curado. En las mezclas con un reemplazo de 3% de nanosílice, se logró un desarrollo de resistencia del 82% (de resistencia final normalizada a 90 días) a los 7 días. Además, se obtuvo un incremento de aproximadamente 40% en la resistencia a la compresión y un desarrollo más rápido de la resistencia mediante la sustitución de una parte del cemento por cenizas volantes y nanosílice en comparación con mezclas que contienen solo cenizas volantes. Pruebas de absorción y permeabilidad fueron realizadas para identificar propiedades que eventualmente pueden tener un efecto sobre la durabilidad del concreto y otras propiedades mecánicas. Los resultados de esta tesis muestran que es posible una mayor reducción en vacíos permeables y absorción en mezclas con mayor contenido

de cenizas volantes y la adición de nanopartículas de sílice. Finalmente, se utilizó un análisis del mercado, los costos y el desempeño del hormigón de alto desempeño para analizar y evaluar los costos del producto para, en un futuro próximo, desarrollar una estrategia de comercialización.

Copyright © by

Hildélix Soto Toro

2017-2018

ACKNOWLEDGMENTS

During these four years of journey preparing for my master's degree, being part of the CREST Project, and the Civil Engineering and Surveying Department, I have been able to meet so many people to whom in some or another way I owe a deepest gratitude. They are so many that I am sure that I will not be able to cover them all here. But there are definitely some key people who cannot go unnoticed.

To begin, I would like to say thanks for the opportunity offered by the Nanotechnology Center, especially the Director, Dr. Oscar Marcelo Suárez whom besides being my thesis Advisor also gave me the opportunity to grow within the Center in unimaginable ways. Always encouraging me, motivating me and placing on my shoulders different challenges and projects that motivate me to grow and explore the unknown. Thanks to those challenges, I left my comfort zone and dared to explore and develop myself in other disciplines such as administration and education. I will never be able to thank him enough for everything he done for my family and me.

I also want to thank the CREST staff members: Myriam, Adelaida, Sylvianne, Boris Renteria and Don Carlos for their great commitment, respect, trust and above all the love they brought to my family from the first day. This team is definitely one of the most challenging, responsible and motivating with which I have had the privilege of working. To my work team and colleagues, without you none of this would have been possible. Nitza, Raul Marrero, Fernando, Carlos Medina, Miguel, Ely, Marivette, Silvia, Cristian, Alfer, Raúl Vega and all those that in some way or another contributed by mixing, making tests, looking for papers and a thousand other tasks. Guys, thank you for all the weekends and holidays in Mayagüez, the long hours of hard work and especially for always supporting me in every project that came up. In general, the entire CREST family, faculty, students and staff are key pieces of this great project that has given me so many opportunities.

In addition, I want to thank all the personnel of the Department of Civil Engineering and Surveying and especially the technicians of the Materials

Laboratory: Monse and Camilo, who always gave me a hand in the laboratory when needed.

Finally, to my family, because without their support, patience and unconditional love, the journey would have been more difficult.

I feel really lucky to have been part of this great team.

To all of you THANK YOU!

To my daughter, Amaia

I wish you the strength to face challenges with confidence. Along with the wisdom to choose your battles carefully. I wish you adventure on your journey and may you always stop to help someone along the way. Listen to your heart and take risks carefully.

Love, mom.

CONTENTS

LIST OF FIGURES

LIST OF TABLES

ACRONYMS AND ABBREVIATIONS USED IN THE RESEARCH

Some terms have been coined to explain process in the present research. The following list explains the expansions of some of the most commonly used acronyms:

Fly ash	FA
Nanoparticles of silica	nS
Portland cement	PC
Superplastizicer	SP
American Concrete Institute	ACI
American Society of Testing Materials	ASTM
Mega Pascals	MPa
Design of experiment	DOE
Compressive strength	f'_c
Splitting tensile	f'_{sp}
Modulus of rupture	f'_r
High performance concrete	HPC
High strength concrete	HSC
Calcium-silicate-hydrate	CSH

CHAPTER I

1 INTRODUCTION

1.1 JUSTIFICATION

In modern concrete technology, reducing cement demand lowers carbon dioxide emissions caused by its production [1]. One option that engineers and researchers are suggesting to reduce this demand in a standardized way is incorporating mineral additives and special materials in substitution of cement into concrete mixtures, classified as high-performance concretes. This particular form of concrete exceeds the properties and constructability of normal concrete and must meet a combination of performance requirements [2].

Nowadays, fly ash (FA), which is an industrial waste product, and microstructured SiO_2 (silica fume) are common mineral admixtures in high-performance concrete mixes. Because of FA low cost, in some places, its use can help lower concrete prices. Unfortunately, due to an ensuing lower reaction, after FA is added in significant quantities, the rate of strengthening of the mix is lessened at early ages. This slower reaction caused by FA motivates the present research on the addition of nanostructured SiO_2 or nanosilica (nS), a modern mineral admixture additive for concrete. In effect, nS is intended to counteract the strength loss to favor a high performance concrete. Recently, with the increasingly research and the reduction of manufacturing costs of the nanomaterials, the use of nanosilica on concrete has received particular attention. It has been shown that the use of nanoparticles in small amounts can improve the performance of HPC by densification of the mixtures and the increase of resistance gain rate when using large amounts of fly ash. Nanomaterials, catalog as a new material, has already shown wide range of potential applications in several industry fields, for example in National Defense.

However, the use of nS in the concrete industry is not yet common and their physical-chemical effects, as well as the resulting mechanical strength and durability, are subject of rising interest. Nanostructured silica, having an average diameter of 69 nm, was used in the present research based on supporting results obtained in a prior study [3], where the use of FA and nS was found to improve

the concrete microstructure and rate of strength gain. Further, scanning electron microscopy examinations in the interfacial transition zone suggested that compressive strengths of nS-containing systems be controlled by both densification and filler effects ([4], [5]).

In the present research and since the study of concretes containing Portland cement (PC), nS, FA, and superplasticizer (SP) can be complex and time-demanding, a design of experiment (DOE) procedure for mixtures was developed. By utilizing a DOE and based on previous optimization strategies ([3], [5]), a design of optimized mixes proportions was achieved. The DOE consisted of an appropriate set of points over an experimental region centered on the strength as a function of the levels of the concrete components, while keeping the water-to-binder ratio constant at 0.3. A maximum of 6.0% of nS was used. Accordingly, the main objective of this research is the analysis of the mechanical tests necessary to determine whether nanoparticles improved the mechanical behavior of concrete when high amounts of fly ash are present. By means of mechanical tests one can determine the most important properties when selecting the materials in the designs, as the main function of the pieces in concrete is to withstand forces. Mechanical characterization, as compressive and tension strength tests, was produced at different age of curing. Tensile results were obtained by two indirect methods of splitting tensile and modulus of rupture (flexural strength) tests. Penetration resistance tests were completed to define the initial and final setting times of the concrete. In terms of durability, absorption and permeability measured by carrying out early age tests allowed identifying the mixes' potential performance when exposed to different chemical or physical attacks. This study intends not only to develop and characterize a high performance concrete bearing nanosilica but to analyze and evaluate costs of the product to, in the near future, develop a commercialization strategy. Consequently, an analysis of the high performance market, costs and concrete performance was used to develop the study.

1.2 OBJECTIVES

1.2.1 General Objective

The objective of this research is to characterize optimized designs of high performance concrete mixtures with the use of high quantities of fly ash, as the mineral admixture, and nanostructured silica as partial cement replacement. As aforementioned, the analysis of the mechanical performance and durability helped identify if the nanoparticles improve the mechanical behavior of the concrete when using high amounts of fly ash. Design mix proportions were designed by the utilization of an optimized design of experiment (DOE) model. Mechanical characterization focused on assessing the compressive strength, splitting tensile strength, and flexural strength at 7, 28, and 90 days of curing. Durability characterization followed to determine the absorption and permeability conditions of the mixes.

1.2.2 Specific Objectives

Part I. Design of Experiment

a. Determine the appropriate set of points over an experimental region of design using a statistical DOE for the mixtures. This DOE centered on the strength as a function of the levels of the concrete components, while keeping water-to-binder ratio constant at 0.3.

Part II. Characterization

Initial characterization test was performed to ensure proper compatibility among admixtures (superplasticizer), mineral admixtures (fly ash and nanostructured silica), and the matrix. In order to obtain the most appropriate admixture proportion for an auto-compacted high performance concrete a mini slump test (ASTM 143 [7]) was performed. An optimal proportion was attained utilizing trial and error evaluation with different admixture proportions in each mix at the fresh state.

To attain these goals, the ensuing mechanical characterization of the five mixes obtained by DOE encompassed the following tests at the hardened state:

a. Compressive (ASTM C39 [8]) and splitting tensile (ASTM C496[9]) strength test at 7, 28, and 90 days of curing using 50 x 101 mm cylinders.
b. Early compressive strength tests (ASTM C39 [8]) at 24, 48 and 72 hours of curing using 50 x 101 mm cylinders.
c. Flexural strength tests (ASTM C78 [10]) at 7, 28, and 90 days of curing using 101 x 101 x 355 mm beams.
d. Penetration resistance test (ASTM C403[11]) to define initial and final time of setting. Initial tests were performed after an elapsed time of 1.5 to 2 h after the initial contact between cement and water. Subsequent tests were conducted at 0.5 to 1 hour intervals.

The third part of this characterization study focused on durability properties:. This was the absorption and permeable pore space test (ASTM C642 [12]) at 7, 14, 28, and 90 days of curing using 72 x 152 mm cylinders.

CHAPTER II

2 LITERATURE REVIEW

2.1 High Performance Concrete

Before any further discussion, one must notice that high strength concrete (HSC) and high performance concrete (HPC) are not synonyms. Normally, HSC is defined based only on the compressive strength obtained at a certain age. The ACI 363 Committee [13] adopted a definition to high strength concrete as: “Concretes with compressive strengths for design of 8000 psi (41MPa) or greater, but for the present time, considerations shall not include concrete made using exotic materials or techniques”.

Both concretes are considered new materials and developments have been gradual over the years. New developments in materials science and technology made possible such growth. These technological advances would satisfy a demand for higher strength concrete when a stiffer structure is required shortly after molding, or when special properties are required. Also, construction element sizes can be reduced leading to streamlined designs, which would require less concrete amount and less formwork. Since these two are the major contributors to the cost of a given project, these new technologies can turn concrete into a more sustainable and environmentally friendly material.

HPC is made with carefully selected ingredients and is based on optimized mixture designs. Here, one must add that there are a number of special concretes with special properties are not referred to as HPC. Examples are underwater concrete, foamed concrete, autoclaved aerated concrete and roller compacted concrete. The main broad divisions of HPC are high strength concrete, high durability, and self-compacting concrete [14].

One of the main ingredients of HPC is finely divided mineral admixtures because of their pozzolanic properties. Mineral admixtures as fly ash and silica fume have been widely used. Significant increase in mechanical properties, better workability (when using fly ash only), and durability are contributions of the admixtures selected [15]–[17]. Plasticizers and other special admixtures are used

to provide workability to the HPC and ease of placement to the mix without affecting the water/cement ratio.

HPC characteristics are developed for particular applications and environments. Some of the properties that may be required include: high strength (in general), high early strength (in particular), high modulus of elasticity, high abrasion resistance, high durability and long life in aggressive environments, low permeability and diffusion, and ease of placement among others [2].

High strength HPC exhibits superior properties and less internal micro-cracking for a given applied axial strain. As a result, the relative increase in lateral strains is lower for high strength concrete[13]. The abrasion resistance, which is directly related to the HPC strength, makes high strength concretes convenient for different abrasive environments, as spillways and stilling basins, or pavements subjected to heavy or abrasive traffic [2]. Nowadays, HPC design focuses more in high durability in severe environments resulting in structures with longer life. For that reason, the introduction of new materials and new technologies in concrete industries is becoming more interesting and crowded, creating a much broader field of study on this type of concrete.

2.2 THEORETICAL BACKGROUND

2.2.1 Fly Ash

Recent concerns about the sustainability of PC, the main ingredient of concrete, has led to the use of concrete supplementary cementitious materials (SCMs), with fly ash being one of the most widely used as partial replacement of ordinary Portland cement (OPC) in concrete. Fly ash, i.e. a reactive aluminosilicate material of industrial origin, is a pozzolanic material. Hence, this waste material must be supplied in a finely divided state or be ground to cement fineness [18]. With the addition of fly ash to the concrete, lower water cement ratios are possible because of its great docility, and a reduction in the heat of hydration due to the decrease in amount of cement. Unfortunately, as aforementioned, when FA is used as a replacement, a slower reaction occurs, adversely affecting the concrete strength at early age (Fig 1). As a consequence, fly ash use is limited to approximately 20-25% by mass in concrete [19].

Fly ash is a by-product that is collected from an electrostatic precipitator after combustion at a pulverized coal firing boiler of a power plant. The molten particles are swept out of the furnace with the stack gasses and collected by the electrostatic precipitators after cooling [18]. Thus, there is an increasing demand for research of fly ash from the viewpoints of environmental pollution prevention and by-product recycling [20]. The use of fly ash helps minimize environmental concern caused by the manufacture of cement that generates large amounts of CO_2. FA can be classified in two classes: class F and class C. Class F, which has aluminosilicate glass as an active component, possesses pozzolanic properties but little or no cementitious properties. The Class C, which has calcium aluminosilicate glass as an active component, has pozzolanic properties and some autogenous cementitious properties.

Some improvement in fluidity has been reported after FA addition. In effect, since FA is lighter than cement, FA prevents cement particle to flocculate, which tends to delay cement hydration and since it bears a spherical shape, it has a ball-bearing effect [20].

When certain mineral admixtures are used, the cost of concrete can be reduced (FA is less expensive that cement, in general) and the properties of mortar or concretes can be enhanced. In some cases, an improvement in early strength becomes apparent, while in others, an increase in late strength occurs.

Toutanji et al. [21] studied the effect of FA and silica fume (SF) on concrete. They found that FA addition caused a reduction in compressive strength as much as 50% with the addition of 30% FA when compared with the control mix (100 % Cement). This reduction is attributed to the slow FA pozzolanic reaction considering that some fly ashes need more than 28 days to develop strength. They also discovered that a combination of different supplementary materials, as silica fume, increased the compressive strength (Figure 1). Previous work support these findings [3],where the use of FA and nS was found to improve the concrete microstructure and rate of strength gain (Figure 2).

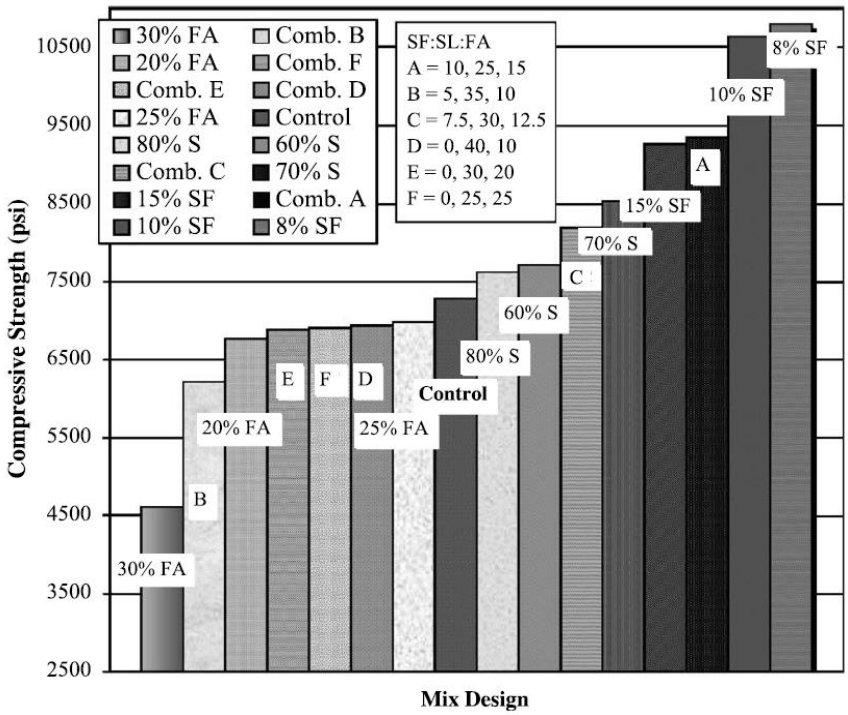

Figure 1: Compressive strength performance at different supplementary materials combinations [21].

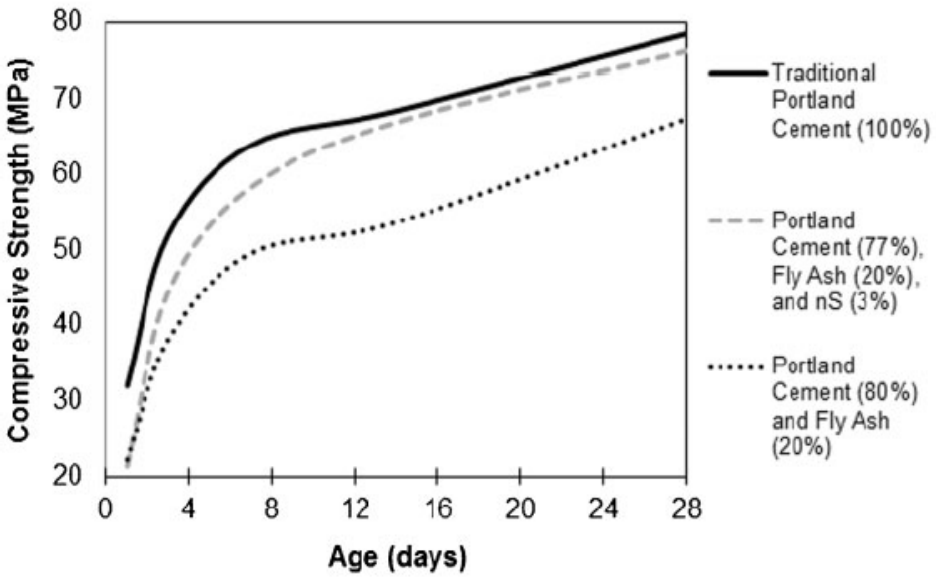

Figure 2: Compressive strength in mixtures bearing different cement proportions as function of mixture age [6].

2.2.2 Nanostructured Silica

Ongoing advances in concrete technology have demonstrated the importance of thorough comprehension of the concrete structure at the nano and the microscale. Understanding the inherent chemical and physical properties and resulting mechanisms can help researchers predict properties and better design concretes for specific applications.

Nanoengineering encompasses the techniques of manipulation of the structure at the nanometer scale to develop a new generation of tailored, multifunctional materials. In our case, nanoengineered concretes are cementitious composites with superior mechanical performance and durability with the potential of bearing a breadth of novel properties [22]. An example of nanoengineered concrete is the addition or partial substitution of cement by nano-sized constituents, such as nanoparticles or carbon nanotubes (Figure 3).

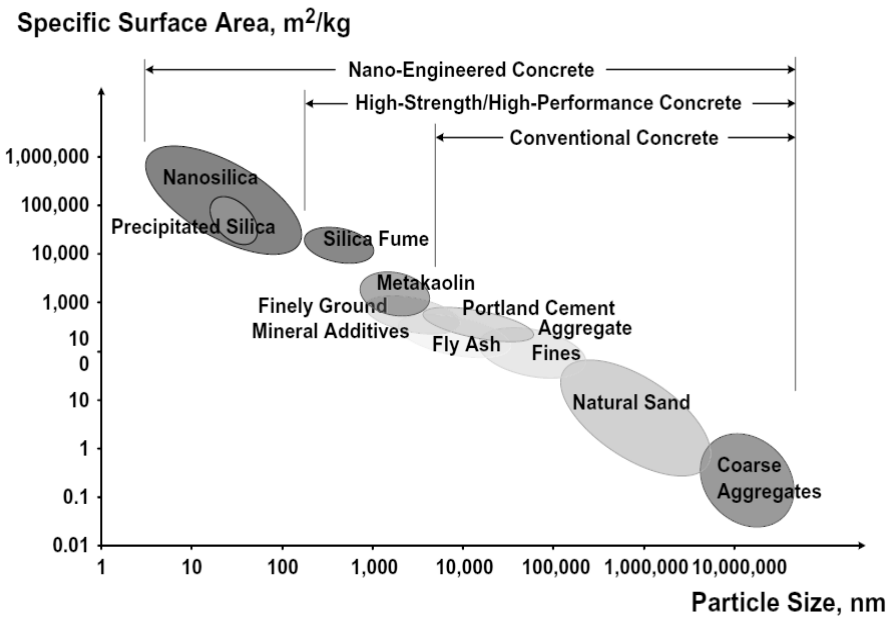

Figure 3: Particle size and specific surface area related to concrete materials [22]

There are many production methods of nanostructured silica. The most suitable for concrete industry is based on a sol-gel process (organic or aqueous route) at room temperature. In this process, the starting materials (mainly Na_2SiO_4 and organometallics as tetramethoxysilane and tetraethoxysilane are added to a

solvent. Subsequently, as the pH of the solution changes, the formation of silica gel occurs. The produced gel is aged and filtered to become a xerogel. This xerogel is dried and burned or dispersed again with a stabilizing agent (Na or K) to produce a concentrated dispersion with 20 to 40 % of solid content, which is suitable for use in concrete fabrication [23].

The main characteristics of nS present in concrete include its high surface area, its water adsorption, and an accelerating effect leading to CSH-gel (calcium-silicate-hydrate) formation. Such high surface area promotes chemical reactivity in concrete, which accelerates the hydration reaction of tricalcium silicate (C_3S) and ash cement, favoring the pozzolanic reaction and the CHS-gel formation [22]. Hou et al. [24] showed that the hydration temperature peak and hydration rate increased with a 5% addition of colloidal nS. Because of the accelerating effect, concretes and mortars with nS tend to require more water to retain adequate workability. For this reason, it is common to use a water reducer or plasticizer to decelerate the effect and make it more manageable [24], [25].

Tricalcium silicate hardens rapidly and is mostly responsible for the initial penetration resistance (initial set time) and early strength. The calcium-silicate-hydrate (C-S-H) keeps the concrete together comprising approximately 50% of the paste volume and affects most of the engineering properties of concrete. Also, due to some chemical incompatibility (structural instabilities) in the materials employed and proportions used, $Ca(OH)_2$ crystals at early and later ages are expected [4]. Equations 1 and 2 show the principal reactions that occurred on this interaction.

Cement reaction: $C_3S + H_2O \rightarrow C\text{-}S\text{-}H + Ca(OH)_2$ (1)

Pozzolanic reaction: $Ca(OH)_2 + \text{Pozzolan} + H_2O \rightarrow C\text{-}S\text{-}H$ (2)

Researchers have already demonstrated that nS can improve the microstructure and reduce the water permeability of hardened concrete. Microstructure analysis of concrete by scanning, scanning transmission, and transmission electron microscopy revealed that nS particles filled the CSH-gel structure voids and acted as nuclei, tightly bonded with the CSH-particles [23]. This tight packing densifies concrete, protecting it from chemical attacks and leaching, while enhancing its

durability and mechanical properties. Nonetheless, the use of nS in the concrete industry is not yet common and their physico-chemical effects, as well as mechanical strength and durability, are subject of rising interest.

CHAPTER III

3 MATERIALS SELECTION, DESIGN OF EXPERIMENT AND CHARACTERIZATION METHODOLOGIES

The following sections describe the materials to be used and the overall experimental procedure of the research project**.**

3.1 MATERIALS

3.1.1 Portland Cement

The main component of the material studied in this research is ordinary Portland cement type I (ASTM C150 [26]), provided by Essroc San Juan, Dorado, Puerto Rico. The specific gravity of PC was 3.1. Table 1 shows the nominal physical and chemical properties of this cement, as provided by the manufacturer.

Table 1: Chemical and physical characteristics of cement type I [27]

Compound	*Measured Amount (wt %)*	*Physical Properties*	
SiO_2	20.8	Loss on ignition	2.6
Al_2O_3	5.3	Blaine (m^2/kg)	429
Fe_2O_3	3.4	Air content (%)	6.7
CaO	65.3	***Compressive Strength (MPa)***	
MgO	1.2	1 Day	13.7
SO_3	2.7	3 Day	25.5
C_3S	59.4	28 Days	42.8

3.1.2 Mineral Admixtures

The type of fly ash to be used is class F (low-calcium) (ASTM C618 [28]) with a specific gravity of 2.4, provided by Essroc Italcementi and Cemex. This class of Fly Ash have very low puzzolanic reaction. However, we decided to use this type of fly ash to develop a greater commercial output.

The silica nanoparticles are supplied as opalescent and odorless amorphous silica dispersed in water and bearing an average particle size of 69 nm, with a specific gravity of 2.0 and an emulsion with a pH of 9.7, provided by Nissan Chemical Industries in Houston, Texas. The amounts of nS in the mixes are calculated based on the percentage by weight of solid in the colloidal solution. In the case of these nanoparticles only 45% by weight is SIO_2. To calculate the amounts of nS for the mixtures, the amount of water and solids is considered, thus making an adjustment to the amounts of both nS and water, in order to then reach the percent established for the design. For instance, the amounts of nanosilica was computed as follows:

Mix Design #1 = (PC:0.54, FA:0.40, nS:0.06)

Total Cementitious quantity: 692 kg/m^3

nS (solids + water) = 92 kg/m3 => *nS (solids) = 92*45% = 41 kg/m^3*

FA = 277 kg/m^3

PC = 374 kg/m^3

Sum (PC +FA + nS(solids))= 692 kg/m^3

3.1.3 Superplasticizer

Because of the accelerating effect on CSH formation, concretes and mortars bearing nS tend to require more water to retain adequate workability. For this reason it is common to use a water reducer or plasticizer to decelerate the hardening effect and make the mixture more manageable [24], [25]. The superplasticizer is a carboxylate polyether-type copolymer (ASTM C494 [29]), commercially designed as a high-range water-reducing admixture (HRWRA) ADVA 575. All doses are expressed as the ratio by weight between the solid active matter and the cementitious content (wt%). Each mixture has a specific proportion of SP with a pH of 5.65 and a 38% solid content provided by Darex Company in Puerto Rico.

3.1.4 Aggregates

The gravel used was a coarse aggregate (grade 7, according to ASTM C33 [30]). Beach sand and processed sand (bearing a fineness modulus of 3.0 ASTM C136 [31]) were added as fine aggregates. The fine and coarse aggregates were oven dried before being used**.** Based on ASTM C127 [32] and ASTM C128 standards, the absorption of the aggregates was 1.6% for gravel and 3.6% for sands. The percent of processed and beach sand were 40% and 60%, respectively.

3.1.5 Water

The source of the tap water used is the system available at the Construction Materials Laboratory of the University of Puerto Rico - Mayagüez.

3.2 DESIGN OF EXPERIMENTS: MIX PROPORTIONS

A statistical DOE for mixtures with extreme vertices was devised to determine the design points for the experiment. This is a special type of response surface experiment in which the factors are the ingredients or components of a mixture, and the response variable is a function of the proportions of each ingredient in the mixture [33]. The vertices of the triangle represent the components that were varied (PC, FA, nS). In the vertices, each material represents 100% of the amount of that material and while moving to the other side of the vertex the percentage goes down until it reaches zero.

Five combinations of cement mixture components were obtained for this design, using Portland cement, fly ash, and nanostructured silica. The levels of the cementitious components were varied to completed a 100% as follows: PC varied from 54-100%; FA varied from 0-40%; and nS amount, from 0-6%. The feasible region can be observed in figure 4.The five combinations were prepared with a superplasticizer at a water/binder ratio (w/b) of 0.30. Table 2 shows the proportions and quantities of the five mixes studied.

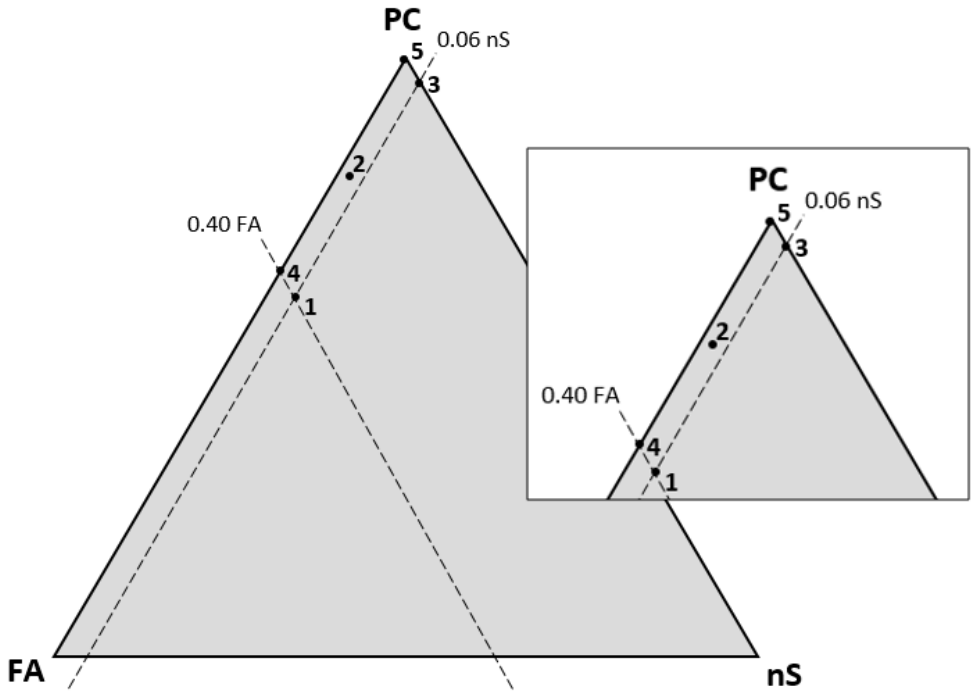

Figure 4: Design points for mixtures proportions obtained from DOE

Table 2: Proportions and quantities of the five mixtures

MN	Mixture Proportions (PC/FA/nS)	PC	FA	nS	Gravel	Sands
		kg/m^3	kg/m^3	kg/m^3	kg/m^3	kg/m^3
1	0.54/0.40/0.06	374	277	92	766	539
2	0.77/0.20/0.03	533	138	46	766	580
3	0.94/0.00/0.06	651	0	92	766	603
4	0.60/0.40/0.00	415	277	0	766	556
5	1.00/0.00/0.00	692	0	0	766	620

3.3 GENERAL MIXING AND EXPERIMENTAL PROCEDURE

Materials were weighed according to the mix design. The water was separated in three equal parts. The coarse and fine aggregates were manually mixed and then placed in the 5L Globe sp-20 mixer, manufactured by Globe Food Equipment, at 110V. Two of the three parts of the water were added over the aggregates. Mixing started at 120 rpm for fifteen seconds. Next, the PC and FA were added over the

aggregates and then mixing continued at 60 rpm for fifteen seconds. At this time nS was added to improve its distribution in the mixture. Afterwards, the SP and the remaining water were added before the last 4.5 minutes of mixing. All molds were then filled and consolidated according to ASTM C192 [34] with the formwork removal occurring 24 hours after casting. Finally, these specimens were cured in limewater for the scheduled aging times. Mechanical characterization as compressive, tensile, and flexural strength tests, as well as early compressive strength and penetration resistance, were obtained at different ages of curing. In terms of durability, we measured absorption and permeability by carrying out early age tests to identify the mixes' possible performance when they are exposed at different chemical or physical attacks.

CHAPTER IV

4 MECHANICAL CHARACTERIZATION OF CONCRETE MIXTURES WITH FLY ASH AND SIO_2 NANOPARTICLES IN THE PRESENCE OF POLYCARBOXYLATE-TYPE SUPERPLASTICIZER

4.1 INTRODUCTION

Concrete is mostly known because of its compressive strength. Consequently, the compressive strength test is the most important characterization test to determine if a concrete mix is reliable. By performing this test, one can determine the potential application of a given concrete, and especially if it complies with the quality and specifications established for a specific use.

Special concretes are of great interest and very complicated to understand at the same time. Hence, this research focused on the mechanical characterization of the experimental concrete mixes. Applying a DOE and previous optimization strategies [3], [5], a design of five optimized mixes proportions was completed. As aforementioned, these mixes incorporated FA and nanosilica as cement replacement.

Both compressive and tension strength tests were completed after different curing ages. Some statistical analysis of compressive strength results were performed using the Minitab® statistical package. In order to assess the reliability of the results obtained in the experiment, parameters such as the mean, p-values, and the coefficient of variation were also evaluated. The correlation coefficient R was used to measure the degree of the relation between the experimental values and the calculated values [35].

Since concrete structures are susceptible to different types of load during their lifetime, we also measured the specimens' tensile resistance. Such failure in tension is governed by micro-cracking, associated particularly with the interfacial region between cement and the aggregates [36]. In ceramics, direct tension without eccentricities is difficult to perform. As a result, there are three methods of evaluate concrete tensile strength, either by direct tension or indirectly by

splitting tensile or flexural (modulus of rupture) tests. Because compressive strength is the principal material property that is measured for hardened concrete, the relationship between tensile and compressive strength is of particular interest. Furthermore, both methods, splitting tensile (f_{sp}) and the modulus of rupture (f_r) are related to compressive strength (f'_c) by equation 3 [18]. The S value is often consider as 0.5 in the literature.

$$f_{sp} \text{ or } f_r = k(f'_c)^S \quad (3)$$

Although flexural tests are not regularly used to characterize a structural concrete, they help us to better understand crack propagation. In this case, the tensile results are required for the design of concrete structural elements subject to transverse shear, torsion, shrinkage, and temperature effects. They are also used in the design of pre-stressed concrete structures, roadways, and runway slabs.

In this thesis, tension results were obtained by two indirect methods: splitting tensile and modulus of rupture (flexural strength) tests. The experimental results of the splitting tensile and flexural strength tests were evaluated and compared with empirical models pre-established in the literature, recommended by researchers or established by codes such as the one by the American Concrete Institute (ACI).

Another property very important for slabs and pavements to schedule finishing operations is the penetration resistance (PR) of a mix. By completing this test, initial and final settings of the concrete can be obtained. According to the American Standards for Testing Materials (ASTM), “the time of setting is the elapsed time from the addition of mixing water to a cementitious mixture until the mixture reaches a specified degree of rigidity” [11]. The cost and performance of concrete impose a massive impact on most construction projects. When dealing with short construction deadlines, the setting time and early age strength of the concrete turns into an essential factor to consider when scheduling a project. Taking this issue into account, when designing the concrete mix in this research, we use FA to reduce the cement quantity, which would lead to lesser construction costs (in some places).

One of the special requirements or properties of high performance concrete is durability that defines serviceability. Concrete durability-related properties are known to be negatively affected due to expansions from freezing and thawing, alkali-aggregate reactions, sulfate attack, corrosion of the reinforcement, etc. Such expansions depend, to a large extent, upon ingress of water, gases, and aggressive chemicals into the concrete; such water ingress, in turn, depends upon permeability (as affected by porosity) [37]. Therefore, absorption and permeability tests allow for a better understanding of concrete durability by analyzing the cement pore system that provides passage for fluid transport into concrete. The materials that constitute the mixture of this high performance concrete are carefully selected to achieve this and other particular properties. Hence, in the present thesis, absorption and permeability were measured by to identify the mixes possible performance when they are exposed to different chemical or physical attacks.

4.2 WORKABILITY

The use of superplasticizers (SPs) is essential for producing adequate workability, but it is important that the binder and the SP are compatible to avoid rapid workability loss. Since the incorporation of amorphous silica has been proved to affect mix manageability, the best proportion of SP-FA-PC-nS was obtained using the mini slump test. This mini slump test (ASTM C143 [7]) was used for the mixtures at 5, 30, and 60 minutes after the mixing along with a trial and error method to found the right proportion of superplasticizer for each mix. The evaluation criteria for slump were from 100-152 mm.

4.3 MECHANICAL CHARACTERIZATION

4.3.1 Early and Late Compressive Strength Test

Concrete strength is calculated by dividing the maximum load at failure by the average cross sectional area. Six 50 x 101 mm cylinders were tested at the same age for each one of the five mixes. The samples were cured in limewater for 1, 2, 3, 7, 28, and 90 days and the average strength was reported in MPa.

4.3.3 Splitting Tensile Strength Test

Eighteen 50 x 101 mm cylinders were prepared for each of the five mixes. The samples were cured in limewater for 7, 28, and 90 days. The universal test machine allowed measuring the splitting tensile strength of the cylinders by the indirect method described in the ASTM C496 [9] standard.

4.3.4 Flexural Strength Test -Third point loading

Four 101 x 101 x 355 mm beams were prepared for each of the five mixes. As mentioned, the samples were cured in limewater for 7, 28, and 90 days. An MTS 810 servo hydraulic testing frame machine allowed measuring the flexural strength of the beams at a constant load applied at a rate of 1.3 mm/min (ASTM C78 [10]). Flexural strength is expressed as the rupture modulus (RM) and the average strength was reported in MPa.

4.3.5 Penetration Resistance Test

Eighteen 50 x 101 mm cylinders were prepared for each of the five mixes. A mortar sample was obtained by sieving a representative sample of the fresh concrete mix. The mortar was placed in the cylinders and stored at ambient temperature. At regular time intervals, the resistance of the mortar to penetration by standard needles was measured with the hydraulic reaction-type apparatus (Figure 5). Initial testing started after 3 to 4 hour measured from the initial contact between cement and water. Subsequent tests should be made at ½ to 1 hour intervals (ASTM C403 [11]). Time intervals between subsequent tests were adjusted as necessary, depending on the rate of setting, so as to obtain the required number of penetrations. At least six penetrations for each time-of-setting test were performed, with time intervals of such duration as to provide a satisfactory curve of penetration resistance versus elapsed time.

Figure 5: Hydraulic reaction-type apparatus used to performed penetration resistance tests

The test continued until at least one penetration resistance reading equaled or exceeded 27.6 MPa (4000 psi). This 27.6 value (final setting) represented approximately a compressive strength of 0.69 MPa (100 psi) [38]. From a plot of penetration resistance versus elapsed time, the times of initial (3.4 MPa / 500 psi) and final setting (27.6 MPa / 4000 psi) were determined.

4.3.6 Absorption and Permeability

Three 72 x 152 mm cylinders were prepared for each of the five mixes. Limewater helped cure the samples for 7, 14, 28, and 90 days. These samples were tested according to ASTM C642 [12], which is the *Standard Test Method for Density, Absorption, and Voids in Hardened Concrete*. This estimates the volume of permeable pore space in a hardened concrete specimen by determining the hardened concrete's mass in different states (oven dry, saturated, saturated-boiled). By using the values of those different masses, as specified in the procedures; we calculated the absorption and volume of permeable pore space (voids).

Table 3: Summary of testing procedure and mechanical characterization

Characterization	Samples (mm)	Standard	Curing Time (days)	Testing Machine
Compressive Strength	50x101 cylinders	ASTM C39 [8]	1, 2, 3, 7, 28, & 90	3000 kN Forney universal test machine (UTM)
Splitting Tensile Strength	50x101 cylinders	ASTM C192 [34]	7, 28, & 90	3000 kN Forney universal test machine (UTM)
Flexural Strength (MR)	101x101x355 beams	ASTM C78 [10]	7, 28, & 90	MTS 810 servo hydraulic testing frame machine
Penetration Resistance	50x101 cylinders	ASTM C403 [11]	Less than 1	Hydraulic reaction-type apparatus (Acme Penetrometer H-4133)Figure 5

4.4 RESULTS AND DISCUSSION

4.4.1 Workability

Table 4 shows the superplasticizer (SP) proportions required for the slump criteria used. Mixes with higher fly ash content, as the MN1 and MN4, showed a lower SP demand. This is explained by the FA's spherical shape that caused a ball-bearing effect. At the same time, MN2 and MN3 mixes showed a higher SP demand. The higher surface areas of the nano-SiO_2 (nS) particles increased the water demand of the mixes. The use of nS increased SP and water demand compared to the control mix. Conversely, the fly ash and nS combination lowered the water requirements.

Table 4: Superplasticizer required for specified slump

Mix Number	Proportions (%nS, %FA)	Superplasticizer (%wt)
1	6, 40	0.4
2	3, 20	0.5
3	6, 0	0.6
4	0, 40	0.2
5	0, 0	0.4

4.4.2 Compressive Strength

Figure 6 presents the compressive strength results after curing the mixes in limewater for 7, 28, and 90 days. In this figure the average of the compressive strength was determined from six cylindrical specimens at each age. Mixtures with nS showed a resistance similar to the control mixture but greater than the mixture containing only FA. The compressive strength of mixes lowered with increasing fly ash levels. Mix MN4 containing 40% FA (the highest level) showed lesser compressive strength. This is because fly ash tends to delay the hydration reaction, decreasing the mechanical properties of concrete at early age although concrete may still continue to acquire resistance at later ages. Nonetheless, mix MN1 with a 40% FA and 6% nS achieved an increase of 38% at 7 days, 27% at 28 days and 20% at 90 days compared to MN4.

Since nS particles are smaller than FA, the pozzolanic reaction (between the SiO_2 in the nanosilica and $Ca(OH)_2$ from hydration products) augmented. On mixes with a 3% nS replacement, an 82% strength gain (of normalized resistance at 90 days) was achieved at 7 days. In addition, a 40% increment (approximately) on compressive strength and a faster development of strength were obtained by a combined cement replacement with fly ash and nanosilica compared to mixtures containing only fly ash (MN4) (Figure 7).

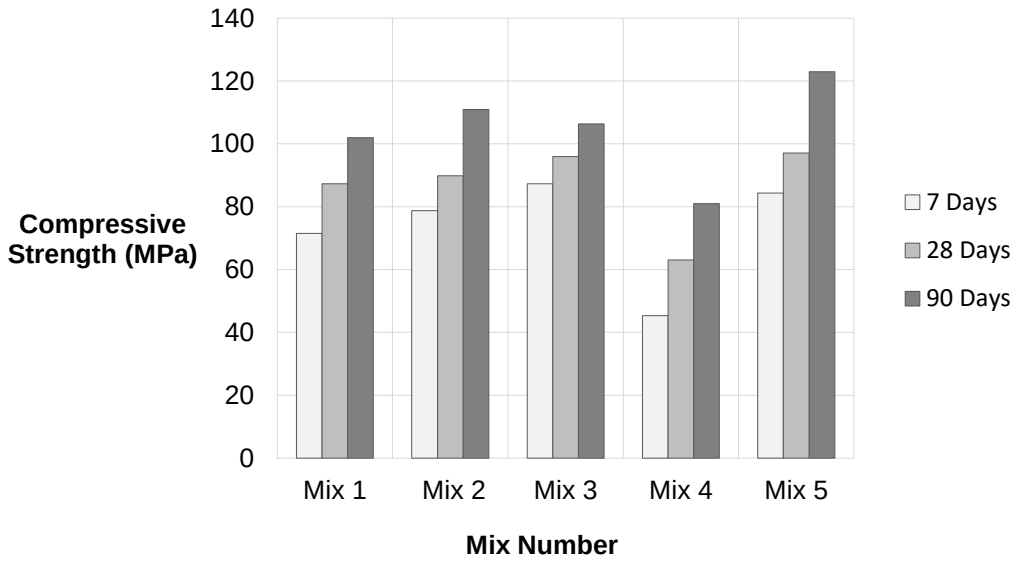

Figure 6: Compressive strength results for mixes test at 7, 28, and 90 days.

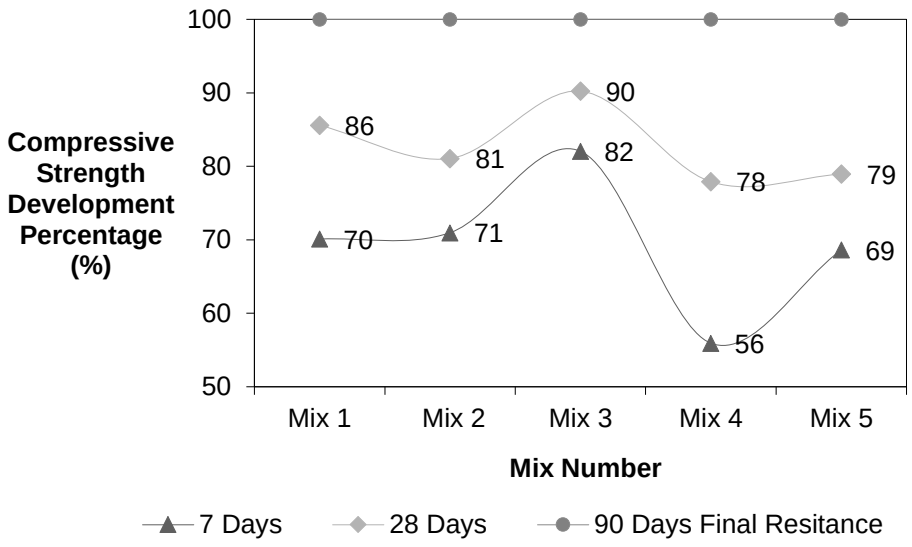

Figure 7: Compressive strength development measured normalized with strength at 90 days of curing.

Figure 8 shows compressive strength results at an early age of 1, 2, 3 and at 28 days. The compressive strength gain rate is acquired slowly in the mixtures with FA. The cement helps to get a faster reaction due to the heat of hydration and can set faster. However, when nanoparticles are used at an early age, a faster strength development is not evident. To catalog a concrete as high early strength, a resistance between 20 to 28 MPa, is necessary at 3-12 hours or 1 to 3 days [2]. Figure 8 shows this resistance was obtained in mixtures with high fly ash content (40%) even before 3 days of curing.

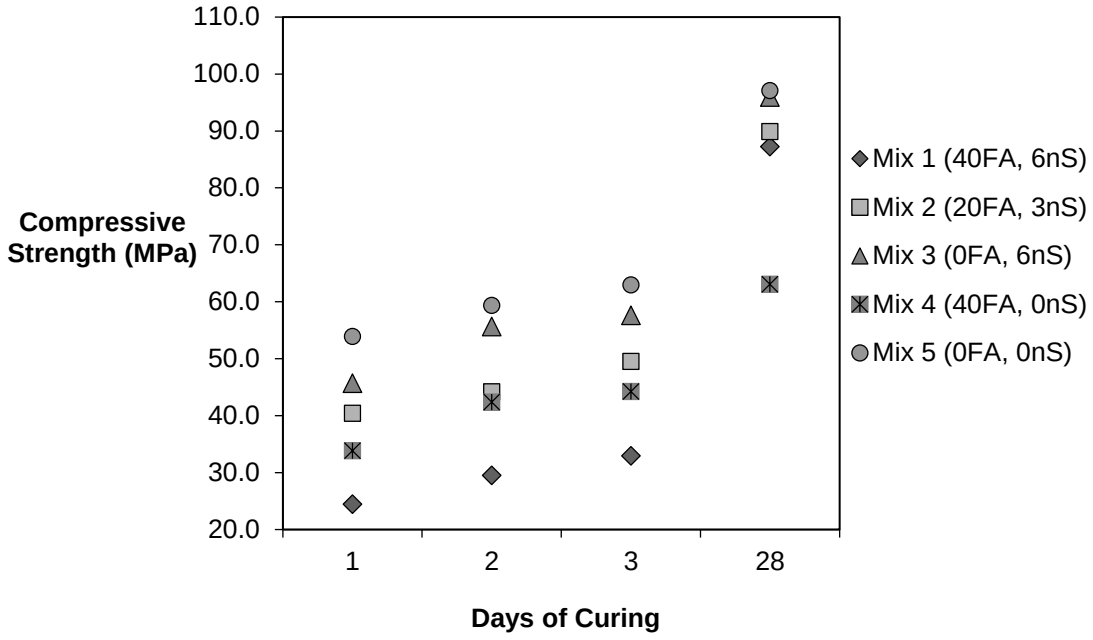

Figure 8: Compressive strength results at 1, 2 and 3 days and a final resistance at 28 days of curing

In this case, fly ash helps concrete to attain resistance in a subtle way, by preventing cracks caused by the rapid reaction due to the high heat of hydration in mixtures of high cement content [15]. The beneficial effect of the nanoparticles is appreciable after 7 days since the concrete with higher contents of FA and 6% of nS acquire a strength resistance 50% greater than when no nanoparticles are present, as previously observed in the compressive results. Accordingly, one can then assert that the addition of nanoparticles leads to a high performance concrete that achieves high strength before 28 days. In addition, one can formulate a concrete that even with a high amount of FA develops an early resistance, high enough to be classified as high early-strength concrete. That classification makes this concrete feasible for more than one application in the field.

4.4.3 Compressive Strength Response Surface Regression Analysis

As mentioned, the experimental design (DOE) helped to investigate the effects of input variables or factors on an output variable or response at the same time. These experiments consist of a series of runs, or tests, in which intentional changes are made to input variables. In this study the input variables are the quantities of nS and FA, whereas the response is the compressive strength. A simple regression analysis revealed variable interactions and individual variable behavior. The effects are statistically significant when their p-values are lower than the level of significance α, in this case 0.05. The complete analysis includes the two main effects and the interaction of 2 factors. Results showed that the most influential effects were caused by the FA level and the interaction between FA and nS. The p-values obtained for quadratic terms (nS*nS and FA*FA) showed a minor or null participation. In other words, nS*nS and FA*FA combinations weren't a meaningful addition to our model, as perceived on the surface response graph in Figure 9. At 28 days the FA level is the most significant factor, as well as its interaction with nS (nS·FA term), with minor participation of nS linear term.

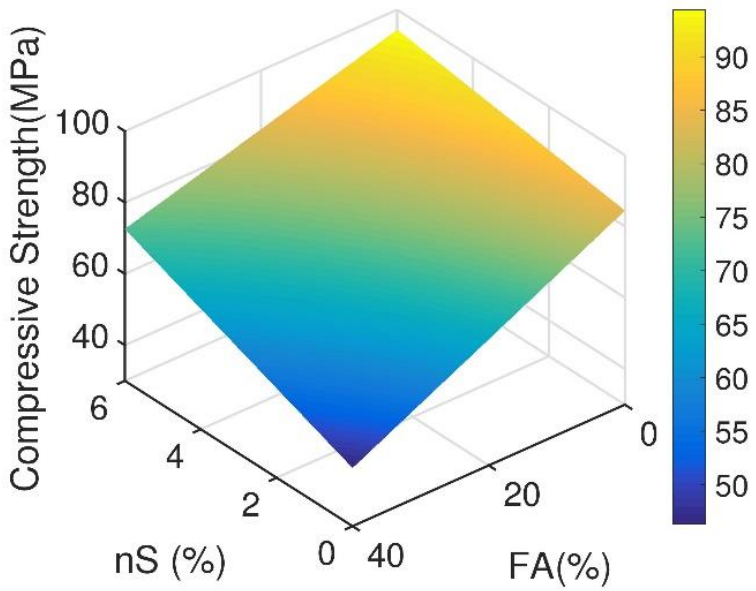

Figure 9: Surface response graph of compressive strength at 28 days for the DOE

The interaction between the quadratic term nS*nS and FA*FA tends to produce multicollinearity. In regression analysis, this occurs when some predictor variables in the model are correlated with other predictor variables [35]. The statistical package used in the analysis, i.e. Minitab®, removed the highly correlated predictors from the model. Results presented a *p*-value from 0.000 to 0.007 with R^2 of 0.9345, 0.9063, and 0.8027 at 7, 28 and 90 days respectively (Table 5). As can be seen nS is not statistically significant by its own at 7 and 28 days of curing.

Table 5: Summary of P-Values and R-Sq % of the DOE analysis at different ages

Age (days)	nS	FA	nS*FA	R^2 (%)
7	0.056	0.000	0.007	93.45
28	0.849	0.000	0.000	90.63
90	0.005	0.000	0.000	80.27

Figures 10 and 11 are contour plots of the effect of each variable (nS and FA) on the compressive strength at 7 and 28 days of curing of the mixes, respectively. One can note that the highest strength is in the lower right corner of the plots, where values of nS fell between 3 and 6% and FA levels, between 0 and 8%. Conversely, the lowest strength values correspond to the upper left corner where lies the maximum amount of fly ash studied in this case (40%) without nS. This was not unexpected since the first detrimental factor for concrete strength is known to be the fly ash levels. As a construction material, concrete offers many possibilities of use; thus, it is important that different ranges of resistance can be obtained as a function of the quantity and nature of the materials available, in this case, the combination of nS and FA.

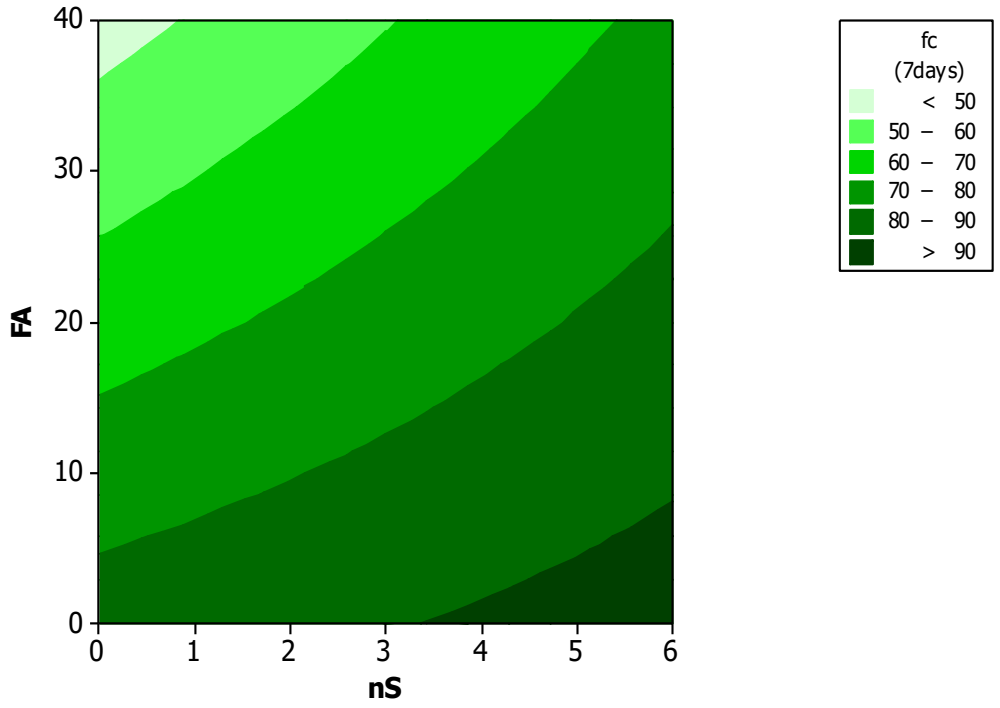

Figure 10: Contour plot for compressive strength (at MPa) at 7 days of curing (i.e. with variation on nS and FA).

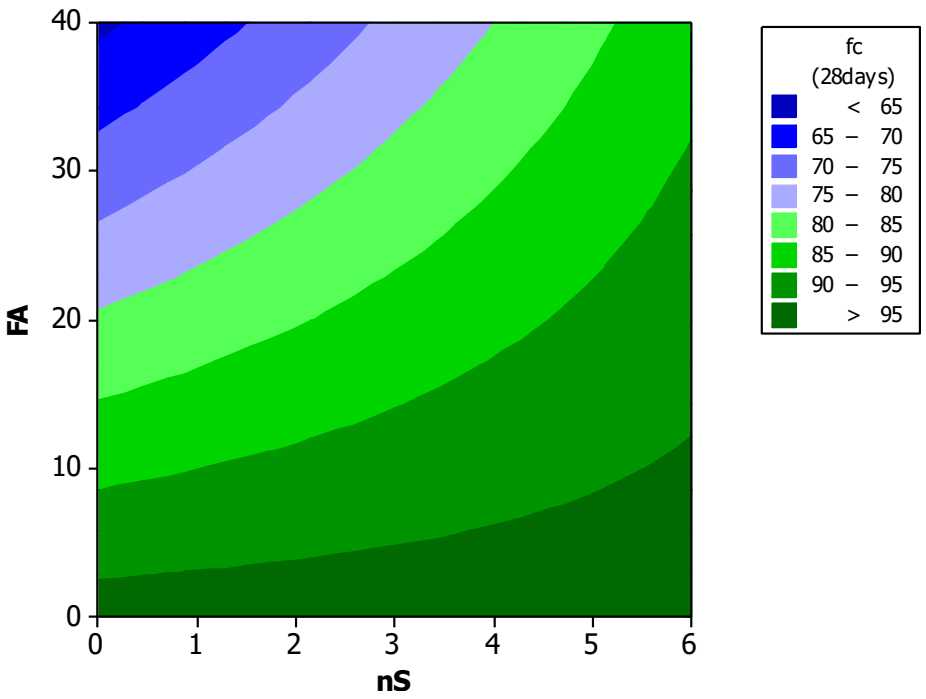

Figure 11: Contour plot for compressive strength (at MPa) at 28 days of curing (i.e. with variation on nS and FA).

4.4.5 Tensile Strength

Splitting tensile strength results were obtained after curing the mixes in limewater for 7, 28, and 90 days. Naturally, the tensile strength values are smaller than the compressive ones (Figures 3 and 4) because cracking propagation by opening mode makes concrete more susceptible to tensile stresses. In concrete bearing nS, the strength gain was higher than or equal to the control mix and an evident strength increase at early age has been attained. At 28 days the maximum values of tensile strength occurred when the nS were present. In addition, the MN1 mix with 40% FA, i.e. the highest replacement level, and 6% nS attained 29% increase at 7 days, 12% at 28 days, and 3% at 90 days, compared to MN4, which has a FA content of 40% and 0% of nS. The MN2 mix, with 20% FA and 3% nS, also displayed a high resistance gain. This significant increase is attributed to the pozzolanic reaction between the cementitious materials. The performance of the mixes with nS on tensile strength was better than the control mix and mixes without nS.

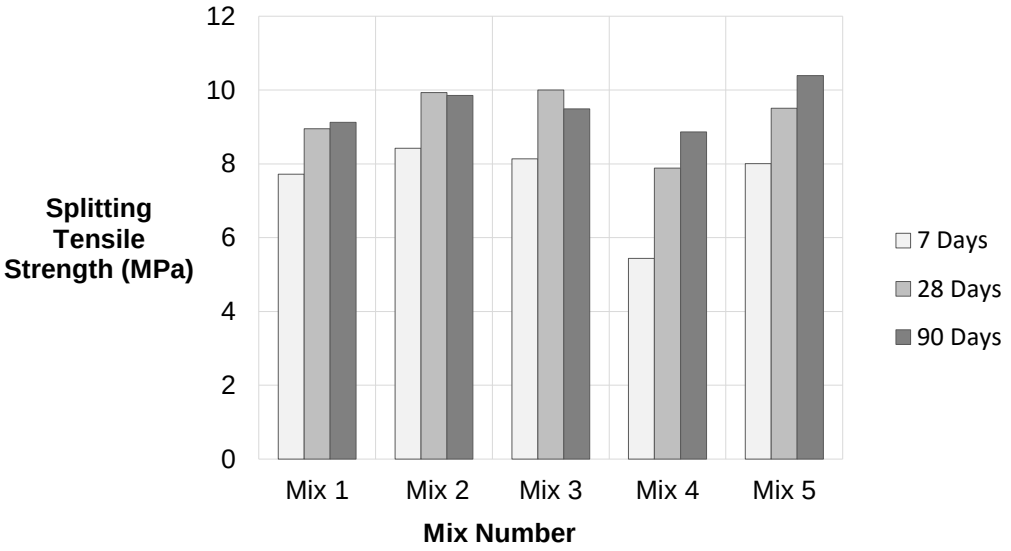

Figure 12: Splitting tensile strength results for mixes test at 7, 28, and 90 days.

Because compressive strength (f'_c) is the principal material property measured for hardened concrete, the relationship between tensile and compressive strength is of particular interest. Here we compared some theoretical and experimental splitting tensile strengths (f_{tsp}). Table 6 shows the relationship

obtained in other studies and the present experimental data. f_{tsp} is the splitting tensile strength, and f'_c is compressive strength, both in MPa.

Equation 4 proposed by Arioglu et al., specifically cover HPC that included silica fume in the mixtures; he also developed similar equations for fly ash additions and other cementitious materials [39]. Equations 5 to 8 were developed by Zain et al., ACI, Iravani, CEB-PIP respectively [39];

$$f_{spt} = 0.321 f_c'^{0.661} \; for \;\; 15 \leq f_c' \leq 120 \; MPa \quad (4)$$

$$f_{spt} = \frac{f_c'}{0.10 f_c' + 7.11} \; for \; f_c' \;\leq 40 \; MPa \quad (5)$$

$$f_{spt} = 0.59 f_c'^{0.50} \; for \;\; 21 \leq f_c' \leq 83 \; MPa \quad (6)$$

$$f_{spt} = 0.57 f_c'^{0.50} \; for \;\; 50 \leq f_c' \leq 100 \; MPa \quad (7)$$

$$f_{spt} = 0.3 f_c'^{0.67} \; for \;\; f_c' < 83 MPa \quad (8)$$

As shown in Table 6, the results obtained from the models reveal a significant difference with our experimental results. The proposed models underestimated the experimental results, thus showing less fragility than expected. These results can be validated with the ratio of both resistances f'_c/f_{spt}, shown in the last column of table 6. Typical values of this ratio are between 0.10 and 0.15 for normal strength concrete (NSC) and lower, 0.06 to 0.08, for high strength concrete (HSC). However, in our results at 28 days this ratio is between 0.10 and 0.12, depending on the mixture. We can justify this strength gain as a result of the high cementitious material quantity.

Table 6: Comparison with relations provided by the literature of splitting tensile strength in terms of compressive strength

		PC/FA PC/SF	**HPC**	**HPC**	**HPC**	**HPC**	Exp. f'spt (28 days)	Exp. f'spt/ f'c
	28 days	15<f'c<120	f'c> 41	21<f'c<83	50<f'c<100			
Mix #	f'c (Mpa)	**Arioglu** [39]	**Zain et al.** [39]	**ACI 363 R-92** [13]	**Iravani** [39]	**CEB -PIP** [39]		
1	87.3	6.2	5.5	5.51	5.33	6.01	**8.95**	0.10
2	89.9	6.3	5.6	5.59	5.40	6.13	**9.93**	0.11
3	96	6.6	5.7	5.78	5.58	6.41	**10.00**	0.10
4	63.1	5.0	4.7	4.69	4.53	4.84	**7.88**	0.12
5	97.1	6.6	5.8	5.81	5.62	6.46	**9.51**	0.10

According to Zain [39], splitting tensile strength does not have a direct proportional relation with f'_c. The ratio of the two strengths (f_{tsp}/f'_c) depends on the general level of the concrete strength. In other words, as the compressive strength (f'_c) increases, the tensile strength (f_{tsp}) also increases, but at a slower rate. When the rate of f_{spt} increased very slow compared to f'_c, is expected that the ratio of the two strengths (f_{tsp}/f'_c) should decreased with time[39]. A study by Deward states that for lower-strength concrete, tensile strength may increase 10% of the compressive strength; however, for high-strength concrete such tensile strength could reduce to 5% [39]. In our case, tensile strength tends to increase with compressive strength, but a reduction is appreciable after 28 days. As shown in Table 7, tensile strength raised up to 11% of the compressive strength in mixes bearing fly ash and nanosilica. This behavior differs from Deward's study, maintaining de relation among 8% and 11% which leads to a high strength tensile strength on the mixes with high FA content.

Table 7: Relation between compressive strength and tensile strength (R)

	7 Days			28 Days			90 Days		
Mix# (FA,nS)	f_{spt} (MPa)	f'_c (MPa)	**R_{tsp}%**	f_{spt} (MPa)	f'_c (MPa)	**R_{tsp}%**	f_{spt} (MPa)	f'_c (MPa)	**R_{tsp}%**
1(40,6)	7.7	71.5	10.8	9.0	87.3	10.3	9.1	102.0	8.9
2(20,3)	8.4	78.7	10.7	9.9	89.9	11.0	9.8	110.9	8.9
3(0,3)	8.1	87.3	9.3	10.0	96.0	10.4	9.5	106.4	8.9
4(40,0)	5.4	45.3	12.0	7.9	63.1	12.5	8.9	81.0	10.9
5(0,0)	8.0	84.4	9.5	9.5	97.1	9.8	10.4	123.0	8.4

Figure 13 shows the relationship between the compressive strength and splitting tensile strength of high performance concrete at 7, 28, and 90 days of curing. The slopes (S) and the intercepts (K) represent the values of the constants in the general equation k *$(f'_c)^S$. From the constants of the regression equations it was shown that the 0.5 power law between splitting tensile strength and compressive strength does not give very accurate relationship for high performance concrete with nanosilica. Based on this experimental investigation, new relationship was developed for this type of concrete at 7, 28 and 90 days as followed respectively:

$$f_{spt} = 0.466(f'_c)^{0.65} \quad (9)$$

$$f_{spt} = 0.9251(f'_c)^{0.52} \quad (10)$$

$$f_{spt} = 1.626(f'_c)^{0.38} \quad (11)$$

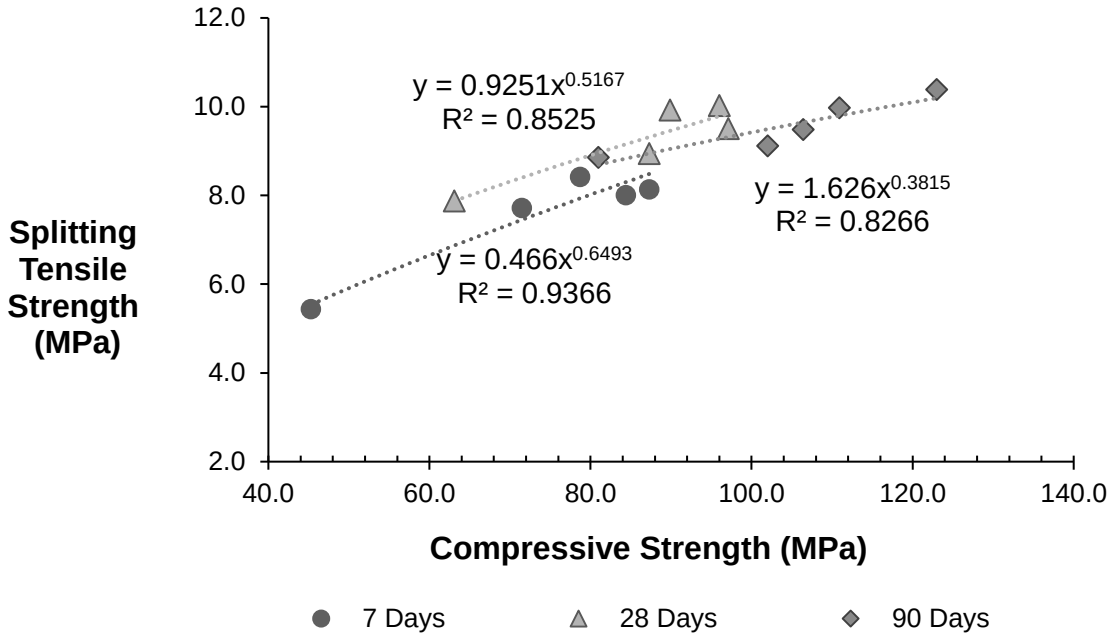

Figure 13: Relationship between the compressive strength and splitting tensile strength of high performance concrete at 7, 28, and 90 days of curing

4.4.6 Flexural Strength

As aforementioned, the flexural strength (modulus of rupture) test is another indirect method for tension strength determination. Since all our beams presented the fracture within the middle third of the light, no test was discarded, as shown in Figure 14. Once again, the tests were completed after curing the mixes in limewater for 7, 28, and 90 days. As expected, the flexural strength values are smaller than the compressive ones. As seen in Figure 15 in concretes with nS the rupture modulus is higher than or equal to the control mix, with a manifest strength increase at early age. However, when the MN4 (40% FA, 0%nS) is compared with MN1 (40% FA, 6% nS), a slightly higher resistance results favored by the nS presence. The maximum f'_r values of at 28 days were found when the mix had nS as in MN3. The MN2 mix (20% FA, 3% nS) also displays a high strength gain when compared to the control MN5.

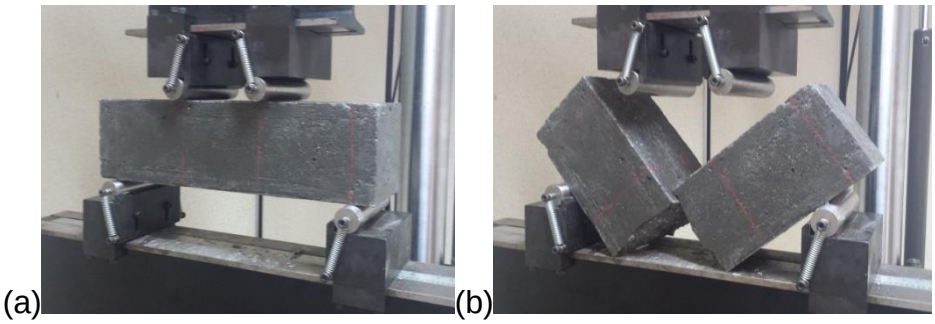

Figure 14: Standard test method for flexural strength of concrete (using simple beam with third-point loading) in the MTS 810 servo hydraulic testing frame machine. (a) Before the test (b) After final fracture.

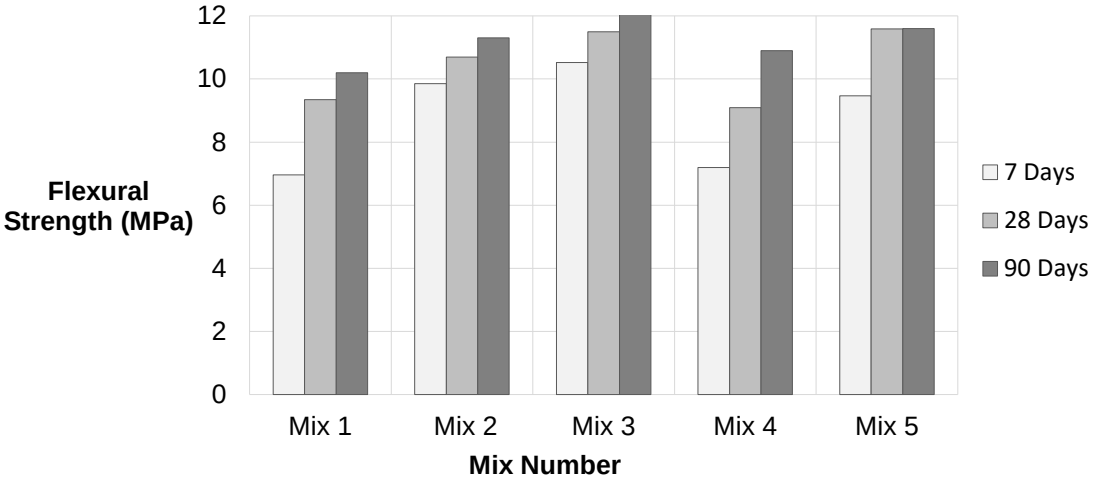

Figure 15: Flexural strength results for mixes test at 7, 28, and 90 days.

As mentioned before, a prior study reported that for concrete with lower strength, tensile strength may attain 10% of compressive strength; however, for higher strength, it could reach only 5%. As shown in table 8, the tendency is that flexural strength falls between 10 and 12% of compressive strength.

Table 8: Percent of flexural strength of compressive strength

	7 Days			28 Days			90 Days		
Mix #	**f_r (MPa)**	**f'_c (MPa)**	**R_f%**	**f_r (MPa)**	**f'_c (MPa)**	**R_f%**	**f_r (MPa)**	**f'_c (MPa)**	**R_f%**
1	7.0	71.5	*9.7*	9.4	87.3	*10.7*	10.2	102.0	*10.0*
2	9.8	78.7	*12.5*	10.7	89.9	*11.9*	11.3	110.9	*10.2*
3	10.5	87.3	*12.1*	11.5	96.0	*12.0*	12.1	106.4	*11.4*
4	7.2	45.3	*15.9*	9.1	63.1	*14.4*	10.9	81.01	*13.5*
5	9.5	84.4	*11.2*	11.6	97.1	*11.9*	11.6	123.0	*9.4*

Table 9 compares some empirical relationship in flexural strengths (f_r) from the literature and our experimental. Here f_r is the flexural strength and f'_c is compressive strength, both measured in MPa. As shown in table, the results obtained from the models reveal a significant difference with our experimental results. As seen the proposed models underestimated the experimental results. Equation 12 proposed by Kothai and Malathy [40] specifically cover self-compacting concrete (SCC). Ahmed et al. studied the effect of different factors on flexural strength and determine that several equations reported in the literature tends to underestimated the resistance. He developed three different equations comprising the square root form, 2/3 form, and effect on depth of the beam. For the sake of brevity, in this study we used the square root form for the comparisons (Equation 13). Equations 14 to 16 were developed in different studies for high strength concrete by Rafael et al., ACI and Logan et al. respectively [40];

$$f_r' = 0.657\, f_c'^{0.5} \qquad (12)$$

$$f_r' = 1.055\, f_c'^{0.5} \qquad (13)$$

$$f_r' = 0.342\, f_c'^{0.5} \qquad (14)$$

$$f_r' = 0.94\, f_c'^{0.5} \qquad (15)$$

$$f_r' = 0.50\, f_c'^{0.5} \qquad (16)$$

Table 9: Comparison of different relations previously developed of flexural strength in terms of compressive strength

	28 days	SCC	HSC	HSC	HSC	HSC	**Exp. f_r (28 days)**	**Exp. f_r / f'_c**
Mix Number	f'_c (MPa)	**Kothai and Malathy**[40]	**Rafael** [40]	**ACI 363R-92** [13]	**Logan et al.** [40]	**Ahmed et al.**[40]		
MN1	87.3	6.1	6.7	8.8	4.7	8.9	**9.4**	0.11
MN2	89.9	6.2	6.9	8.9	4.7	9.0	**10.7**	0.12
MN3	96.0	6.4	7.2	9.2	4.9	9.4	**11.5**	0.12
MN4	63.1	5.2	5.4	7.5	4.0	7.1	**9.1**	0.14
MN5	97.1	6.5	7.2	9.3	4.9	9.5	**11.6**	0.12

4.4.7 Penetration Resistance

The Figure 16 data suggest an inverse proportionality relation between PC quantity and setting time. This made the mixtures with the highest PC concentrations set earlier than those with lower concentrations. Still, the difference between the setting times of some mixes was not considered significant. This can be clearly appreciated between the MN1 and MN4, where MN1 has 6% of its cementitious materials replaced by nS particles. A half-hour difference between setting times proves not to be a big handicap considering that nS provides other mechanical enhancements to the mix [1].

An initial setting time was established at 3.45 MPa (500 psi) [2], while the final setting time was set at 27.58 MPa (4,000 psi) (according to ASTM C403 [11]). An average setting time was determined after testing 3 samples every 30 minutes, until the average reached the established final setting time: 27.58 MPa (4,000psi). This 4,000 psi benchmark represents approximately 100 psi [38] of compressive strength. All mix designs reached a satisfactory setting time when compared to the theoretical setting time range (from 4 to 12 hours) [2], as in Figure 17.

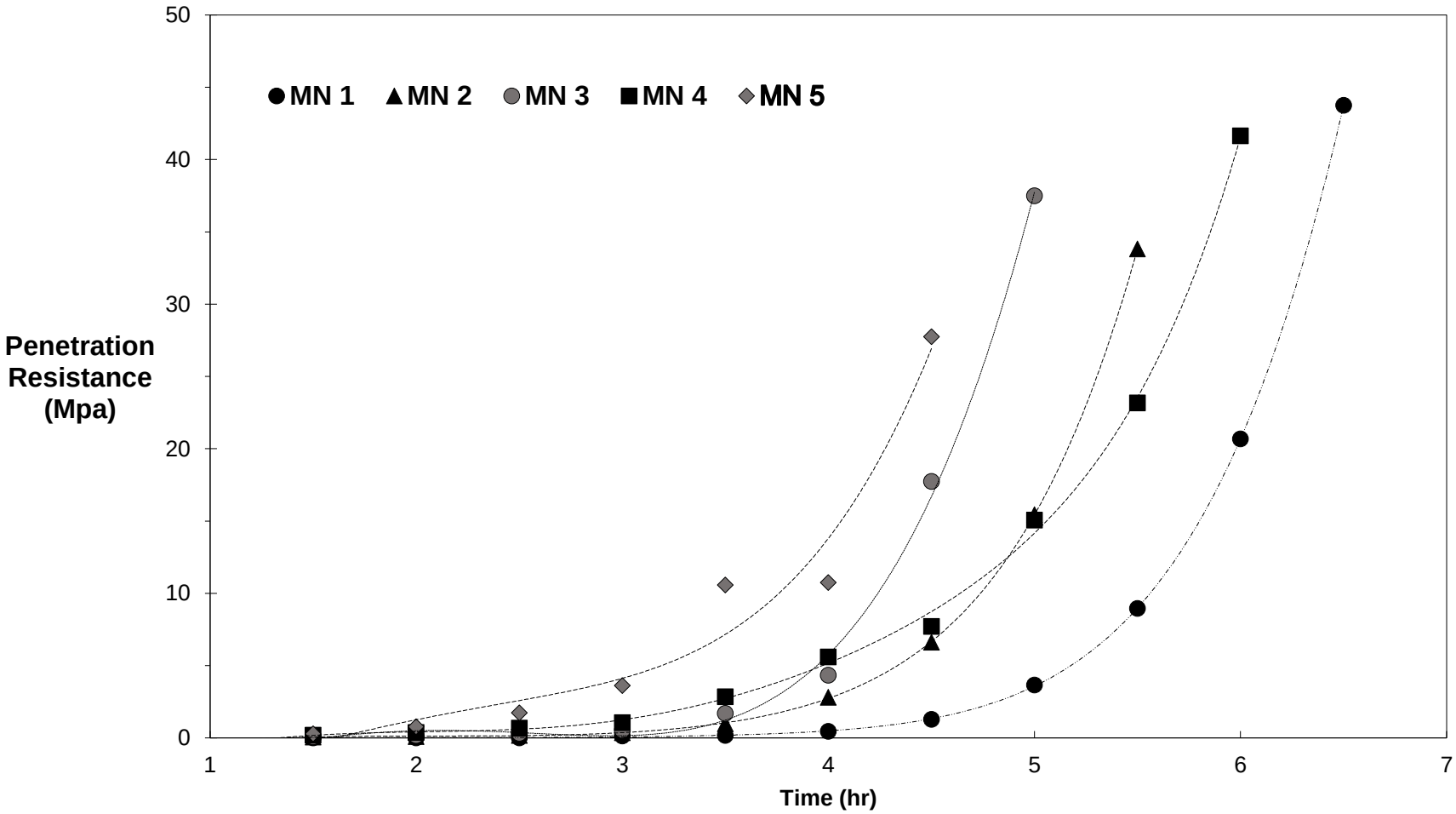

Figure 16: Setting time curves for mix designs.

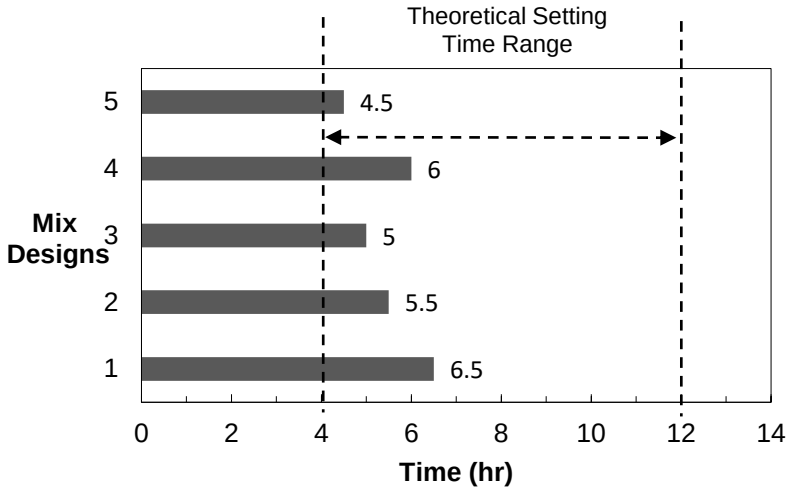

Figure 17: Final setting time.

This proves that the inclusion of FA, nS, and their combination did not necessarily delay the final setting time of the mixes. Therefore, this setting time is not enough to let one consider the concrete a quick setting one.

4.4.8 Absorption and Permeability

Figures 18 and 19 show the results of the water absorption and permeable pore space tests for concrete mixes with constant 0.30 water-to-cement ratio at different curing ages. Higher absorption is evident in the MN4 and MN5 mixes that did not have nS; this leads to more permeable voids in the mixes. Conversely, MN1, MN2 and MN3 mixes that did have nS showed less permeable voids and lower absorption. As mentioned, pores in the cement matrix are responsible of fluids transport or accumulation into concrete. One can observe that the water absorption levels decreased for higher amounts of FA and nS. As expected, the water absorption of MN5 (control mix) and concretes in general rises as the curing time progresses. Upon curing, nS beneficial effect in reducing water absorption became noticeable due to the filler effect of ultrafine particles and to the FA pozzolanic reaction. A higher reduction on permeable voids and absorption is noticeable on mixes with higher FA and nS levels. Therefore, with a 40% FA and 6% nS replacement the filler effect became most apparent. However, with a 20% FA replacement, i.e. the maximum recommended amount in construction field, and in the presence of nS, it is only obtained equal or lesser permeable voids than with higher FA levels (without nS). High performance

concrete (HPC) absorption standards are specified as 2% to 5% [2]. Since our results are within 1% to 3%, our concrete mixes meet the HPC standards.

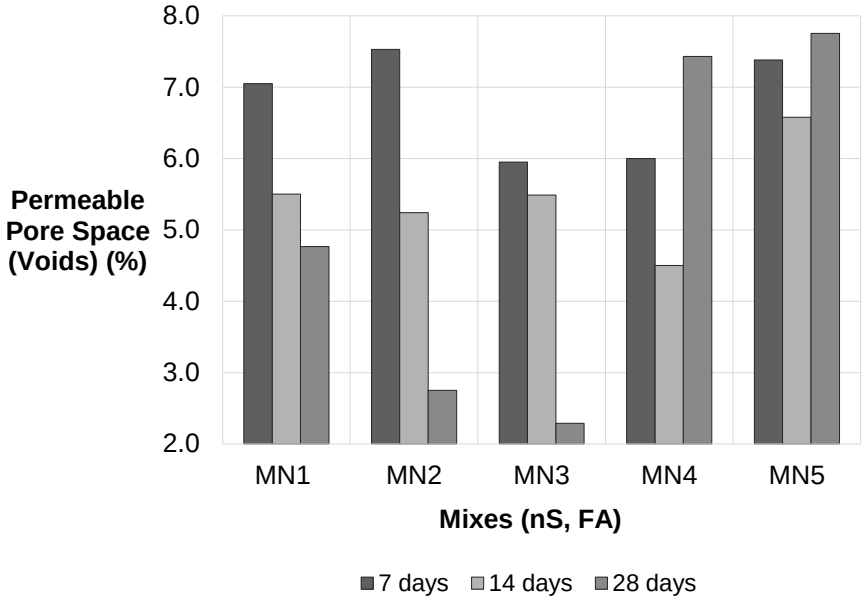

Figure 18: Permeable pore space results for 7, 14, and 28 days of curing

Additionally, our results revealed that both absorption and permeable pores had no apparent relationship with the compressive strength for the range of variables studied. The specimens showed less absorption and permeable pore space on mixes with higher replacement of FA and nS, but at the same time showed higher absorption and permeable pore space on mixes with high compressive strength as the control mix. However, over time this can become an important long term issue because if the concrete is more permeable and absorbent, it could lose its mechanical properties and deteriorate faster than the less permeable concrete.

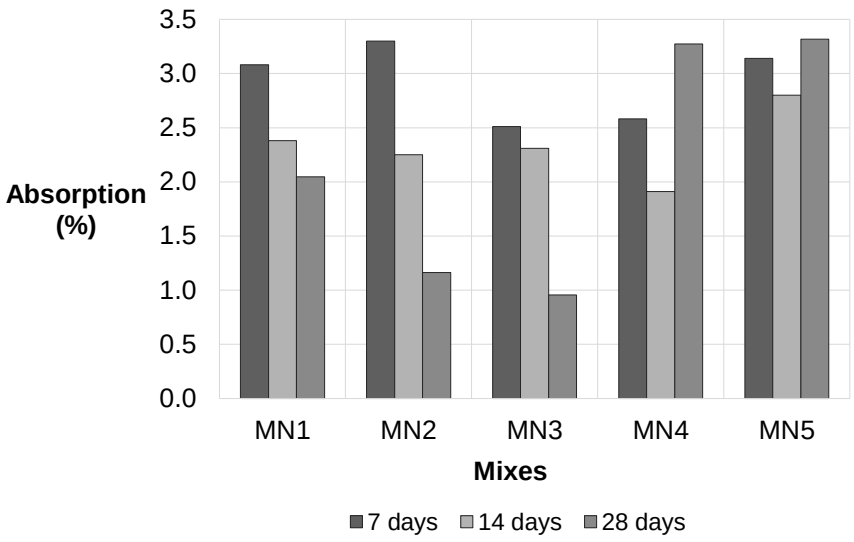

Figure 19: Absorption results for 7, 14 and, 28 days of curing

This reduction in the water absorption with age indicates superior performance of the FA-nS blended cement concretes over the ones without nS. This may be explained by the high hydration reaction of the nS. It is well known that the these reactions contribute to the refinement of the binder capillary porosity, with direct consequences on the improvement of the concrete durability [3].

CHAPTER V

5 MARKET AND COMERCIALIZATION ANALYSIS OF CONCRETE MIXTURES WITH FLY ASH AND SIO_2 NANOPARTICLES PARTIAL REPLACEMENT

5.1 INTRODUCTION

High performance concrete (HPC) has very specific requirements that define their characteristics and uses. To create the mixtures, the materials to be used must be selected carefully. Nonetheless, selection of suitable ingredients for concrete having the preferred rheological properties, strength, and durability could be costly and time demanding. One of the most important properties of this concrete type is that it is self-compacting. This reduces cost related to skilled labor and equipment, while allowing for faster execution and lower noise during placement (no vibration damping required), less defects, less re-work of parts and smaller cost for finishing. In addition, quality control is better due to the complexity of designs and materials. All of these factors cause that HPC be expensive although its use may lead to overall structural economies. A major advantage is that environmental construction sites and precast works are much less noisy, and the health risks associated with handheld vibrators are eliminated. Other very expensive and common factor on HPC or Ultra HPC is high temperature curing method which helps to obtain fast mechanical strength gain. Z. Wu et al. study different curing temperatures and compared the results with room temperature curing methods but with the incorporation of different pozzolanic materials while seeking to obtain same benefits but at lower cost. One of the most important applications of their findings was the satisfactory mechanical properties from using high amount of pozzolanic materials [41]. Using pozzolanic materials eased the applications of HPC and at the same time reduced costs and energy consumption.

The high urbanization rate in densely populated countries, especially China and India, is boosting demand for skyscrapers[42]. This encourages the growth of the high-performance concrete market. As a result, HPC is being considered. Moreover, the rising demand for high-tech railway network is expected to drive

the demand for railway bridges, which is likely to expand the global high performance concrete market in the upcoming years [43].

Recently, with the increasingly research and the reduction of manufacturing costs of the nanomaterials, the use of nanosilica on concrete has received particular attraction. Nanomaterials catalog as a new material has already shown wide range of potential applications in the industry fields as for example in the National Defense. By seeking to enhance the sustainability of the concrete with the nanoparticles or nanomaterials without sacrificing the mechanical properties those nanostructured materials can become more widely used [44]. However, there still high cost is one of the things that increases uncertainties of its use in the construction industry. Although silica is one of the most abundant minerals on earth, it is difficult to control its shape and size. The transformation from its natural state to a stable size requires various synthetic routes as ion exchange from sodium silicate, hydrolysis and condensation from tetraethoxysilane (TEOS), milling or dispersion from fumed silica or silica gel and direct oxidation from silicon that make it expensive [45].

This chapter intends to analyze and evaluate costs of the High Performance Concrete with nS with the vision of a commercialization possibility.

5.2 COST EVALUATION

High performance concrete provides endless mechanical advantages and durability in general constructions. However, given their high initial cost and complexity, they have a low development ratio in U.S. Currently, the cost of a high performance concrete with added fiber is around \$2,600/m^3 (\$2,000/yd^3) in the United States [46]. This commercially available ultra-strength HPC is approximately 20 times more expensive than conventional concrete, which is about \$130/m^3 (\$100/yd^3) [47]. Like any product in development, some costs linked to its high price are the investigation, analysis and selection of its materials, and the training of personnel and familiarization with its process and manufacture. The research of new products, the maturity of the technology, and the development pilot projects is expected to be an important factor in increasing the competition and the mass demand of its production.

In order to analyze the costs of our mixtures it was necessary to look in the properties and significance of the selection of materials in them. As indicated before, our HPC incorporated traditional materials such as cement, sand and stone, as well as supplementary materials such as fly ash and nanoparticles. In addition, a superplasticizer of high quality and compatible with our mixture matrix was used.

We collected prices from different places in Puerto Rico to calculate average prices of the materials. The different prices came from sources as Essroc Italcementi, Cemex, hardware stores, aggregates and chemical suppliers. In Puerto Rico, there is plenty of FA produced by an electrical plant that lacks minimal quality. Therefore, there is restricted access to high quality FA that can only be imported. For this reason, the cost of fly ash found was basically the same as cement, even though it is a bio-product of the burning of coal to produce energy. Table 10 shows the average prices in Puerto Rico for the different materials used and the cost of the nanoparticles of silica (nS) obtained from the mainland. The cost of nanoparticles does not include freight charges. It is apparent that the high nS price is a main factor in the mixing cost. In the US and countries like China and India, there is ready access to fly ash or other supplementary materials at lower cost, regularly lower than cement, in the case of fly ash.

A study by the Federal Highway Administration (FHWA) compared different price ranges for materials that are regularly used in high-performance concrete and develop an optimization process to obtain the best overall cost of a mix for different US regions. Table 11 provides the different price ranges obtained from different regions including New York, Connecticut, New Jersey, Iowa, Minnesota, Michigan, and the Northwest area nigh Washington [47]. Using US prices this FHWA study offers a model able to optimize the use of materials for the development of HPC in those US regions. In the analysis, rates ranging from \$605.2/m^3 to \$852.3/m^3 were computed for different areas, depending on the materials costs for each region [47].

Table 10: Material average cost from different sources in Puerto Rico and nanoparticles of silica from the US.

Material	**$/kg**	**$/Ton**
Cement	0.17	154.22
Fly Ash (Class F)	0.20	181.44
Silica Fume	2.00	1,814.37
Nanosilica (Nissan Chemical Texas US)	10.00	9,071.85
Coarse aggregate	0.02	18.14
Sand	0.03	27.22
Water	0.01	9.07
High-range water reducing admixture (ADVA 575)	$ 14.00 /gal	$ 14.00 /gal

Table 11: Material cost ranges obtained from selected US areas [47]

Material	Ranges		Average ($/Ton)
	Max. ($/Ton)	Min. ($/Ton)	
Cement	250.00	92.00	171.00
Supplement Materials	879.00	46.00	462.50
Silica Fume	1,100.00	350.00	725.00
Coarse aggregate	19.00	8.25	13.63
Sand	162.50	8.50	85.50
High-range water reducing admixture (gallon)	20.00	13.00	16.50

Nanoparticles are not a by-product and are synthesized in a laboratory. For this reason, their cost is high. In the present research, we used colloidal nanoparticles, dispersed in water because, in addition to provide a better dispersion of particles in the mixture, the colloid lowers the risk of inhalation. Colloidal silica can be prepared by various methods and starting materials. Some of these methods include ion exchange of aqueous silicates, hydrolysis and condensation of silicon compounds, direct oxidation of silicon, and milling and peptization of silica powder [45].

Table 12 shows the analysis of different mixtures available in the market or that have been used for existing structures in some part of the world. The study included mixtures like the one used for the Wacker drive bi-level roadway in Chicago completed in 2001, the typical mixture of HPC that appear in the *Design*

and Control of Cement Mixtures textbook, and the mixture designed in the study of Yousry El Shikh for an HSC [2], [48].This comparison revealed that the most influential prices are those of cementitious materials and their replacements such as fly ash and nanoparticles or silica fume. The analysis took into consideration the compressive strength reached at 90 days, calculating the price per unit of resistance ($ / MPa). When comparing them with PR prices one can see that the cost per resistance varies between 2.46 and 5.86 $/MPa depending on the application and materials.

Table 12: High Performance concrete mixes comparison

		Wacker Drive bi-level roadway, Chicago, 2001		**Design and Control OCM** [2]		**HSC-Yousry El Shikh** [48]		**HPC Early Strength (This study)**		**HPC (Prev. Study) Zapata et al.** [3]	
w/cm	**P.R. Prices**	0.3		0.32		0.25		0.3		0.3	
f'c (28days) MPa		-		85		120		90		-	
f'c (90Days) MPa		**60**		**92**		**-**		**110**		**70**	
Slump (mm)		61		203		120		100-150		100-150	
Materials	**$/kg**	**Q**	**$/m³**	**Q**	**$/m³**	**Q**	**$/m³**	**Q**	**$/m³**	**Q**	**$/m³**
Cement Kg/m³	**0.17**	398	67.6	327	55.6	500	85.0	533	90.6	369.6	62.8
Fly Ash Kg/m³	**0.20**	45	9.0	87	17.4	0	-	138	27.6	96	19.2
Silica Fume Kg/m³	**2.00**	32	64.0	27	54.0	50	100.0	0	-	0	-
Nanosilica Kg/m³	**10.0**	0	-	0	-	0	-	46.1	461.0	14.4	144.0
Coarse aggregate Kg/m³	**0.02**	1030	20.6	1121	22.4	1156	23.1	766	15.3	766	15.3
Sand Kg/m³	**0.03**	705	21.2	742	22.3	650	19.5	578	17.3	578	17.3
Water Kg/m³	**0.01**	145	1.4	141	1.4	135	1.3	178	1.8	144	1.4
HRWR l/m³	**3.42**	3	10.3	9.54	32.6	19.3	66.0	9	30.8	8.5	29.1
Total $/m³			**$ 194.1**		**$ 205.7**		**$ 294.9**		**$ 644.4**		**$ 289.1**
$/MPa			**$ 3.24**		**$ 2.24**		**$ 2.46**		**$ 5.86**		**$ 4.13**

w/cm = water and cementitious material ratio
f'c - Compressive Strength
Q- Quantity
HPC-High Performance Concrete
HSC-High Strength Concrete
HRWR-High Range Water Reducer

The construction industry has a very large market as well as an outstanding and important market development capacity. High performance concrete has definitely impacted and will continue to impact the industry by improving the durability of structures and thus their service life. Nevertheless, one must recognize that the costs of materials are not the only determinants in meeting the needs of a project. Even so, the initial cost of the project is a very important factor. The analysis and development of new materials have helped us to improve their performance and develop durable and reliable technologies. In particular, the study of nanoparticles in concrete has expanded rapidly and has been incorporated into the construction industry. For this reason, it is expected that their prices would begin to fall as demand increases. In the meantime, before the decision-making process, it is best to develop a complete cost analysis of the project incorporating the needs and priorities of the project.

CHAPTER VI

6 GENERAL CONCLUSIONS

Based on the results and the discussion of mechanical properties, absorption and permeable pore space obtained in the present research, the following conclusions were drawn.

First and foremost, as expected, the addition of large amounts of fly ash as replacement in the mixtures has appreciable consequences in all strength performances. A slower gain rate of mechanical strength is also considerable, confirming results in the reviewed literature.

Nonetheless, the addition of small amounts of nanostructured silica promotes a significant strength increase in the mixtures containing fly ash. In this nanomodified concretes, the compressive strength values obtained exceeded the values established by ACI for high strength concrete in just the first 7 days of curing, thus improving the strength of concrete with fly ash replacement at an early age. The use of SiO_2 nanoparticles enhances the mixes, allowing them to achieve resistances with similar or higher levels than the control mix in a shorter amount of time, accelerating concrete strength gain, which is one of the primary concerns of the use of high volume fly ash in concrete.

This research also proved that at early curing ages, the nanosilica-containing mix designs did not display a notable improvement in compressive strength and setting time when compared to the other mix designs. The 3-day curing period and each mix's setting time proved to be too short for the nS to properly react within the concrete matrix. Nevertheless, this provides the concrete with a good workability time before suddenly gaining resistance after 3 days of curing. This finding could be critical for the construction crew by not only helping the formwork production but also by substantially shortening the demolding time.

The penetration resistance tests showed that, even though Portland cement is the predominant cementitious material when reducing setting time, none of the mix designs surpassed 6.5 hours before setting, staying well within the lower margin of the required final setting time range set by the Portland Cement

Association. This proves that concrete incorporating FA and nS as partial cementitious replacements can have a somewhat beneficial setting time that would be highly valuable, especially in large scale productions and projects where formwork removal is critical.

At different curing ages, mixes containing fly ash and nanoparticles, bear considerably smaller amounts of permeable pore spaces and absorption levels. Also, the greatest discrepancies in porosity data between both curing times (7-14 days) occurred in the mix designs containing fly ash. This suggests that these particular concrete mixes require more curing time to reach further reduction in porosity and therefore reach higher strength than mixes that do not. At different curing ages, mixes bearing fly ash and nanoparticles we also found that such admixture combination reduces substantially the permeable pore spaces and absorption. By reducing the permeability and absorption of mixtures, better durability is achieved because of the reduction in transport properties through the concrete. For this reason, concrete becomes less vulnerable to chemical attack and steel corrosion.

Considering different property measures, the combined use of fly ash and nanosilica is recommended to obtain a high performance concrete. This is because a mixture with mineral admixtures will be equally or most efficient than a control mixture with just PC, when special concrete properties are considered. Consequently, this research demonstrates unequivocally that a high amount of fly ash replacement is feasible for a concrete mix as long as nanoparticles are present. This formulates a mixture that is not only stronger but also of higher quality and durability.

In closing, high-performance concrete mixtures with a reduced setting time and enhanced mechanical properties were developed. In general, the study of these designs has provided positive results regarding the use of nanoparticles as replacement material in high performance concrete. Special properties such as high early strength, high tensile strength, low porosity and excellent workability are some of the most outstanding findings. The material exhibited remarkable durability and resistance, and surpassed all the specifications established by standards, making it ideal for commercialization and industrialization purposes.

With a more favorable access to nanoparticles, concrete production with special properties, and without high maintenance and commissioning costs is possible.

NEW AVENUES FOR RESEARCH

During the development of this thesis, a breadth of projects and ideas came forth as applications of ecologically friendly concretes. One of the new concrete mixes, which also included nanosilica, incorporated a natural fiber to better the tensile strength of the material and, at the same time, lower the fabrication costs. This segment with potentials for further development is included in Appendix A. The natural fiber used was bamboo as reinforcement. Another project that branched off from the core of this thesis was the use of disposed plastics as an aggregate to concrete. In this case we formulated an *Eco-Brick* or mixture for non-structural constructions, as presented in Appendix B. We understand that both new materials have demonstrated promising features related to sustainability in the construction industry.

REFERENCES

[1] C. Chen, G. Harbert, Y. Bouzidi, and A. Jullien, “Environmental impact of Portland cement production,” in *Cleaner Production*, Elsevier, 2010, pp. 3–25.

[2] W. C. Kosmatka, Steven H.; Kerkhoff, Beatrix; and Panarese, *Design and Control Design and Control of Concrete Mixtures*, 14th ed. Illinois, USA: Portland Cement Association, 2003.

[3] L. E. Zapata Orduz, “Rheological and Mechanical Characterization of Portland Cement Mixes Containing Micro and Nano Amorphous Silica Particles,” Ph.D. Dissertation, University of Puerto Rico, Mayaguez, PR, 2013.

[4] L. E. Zapata, G. Portela, O. M. Suárez, and O. Carrasquillo, “Rheological performance and compressive strength of superplasticized cementitious mixtures with micro/nano-SiO2 additions,” *Constr. Build. Mater.*, vol. 41, pp. 708–716, Apr. 2013.

[5] E. Ghafari, H. Costa, E. Júlio, A. Portugal, and L. Durães, “The effect of nanosilica addition on flowability, strength and transport properties of ultra high performance concrete,” *Mater. Des.*, vol. 59, pp. 1–9, Jul. 2014.

[6] N. M. García, L. E. Zapata, O. M. Suárez, and M. Cabrera-Ríos, “Effect of fly ash and nanosilica on compressive strength of concrete at early age,” *Adv. Appl. Ceram.*, vol. 114, no. 2, pp. 99–106, Feb. 2015.

[7] ASTM Standard C143, “Standard Test Method for Slump of Hydraulic-Cement Concrete,” *ASTM Int.*, pp. 1–4, 2005.

[8] ASTM Standard C39, “Standard Test Method for Compressive Strength of Cylindrical Concrete Specimens,” *ASTM Int.*, pp. 1–8, 2004.

[9] ASTM Standard C496, “Standard Test Method for Splittling Tensile Strength of Cylindrical Concrete Specimens,” *ASTM Int.*, pp. 1–5, 2004.

[10] ASTM Standard C78, “Standard Test Method for Flexural Strength of Concrete (Using Simple Beam with Third-Point Loading),” *ASTM Int.*, pp. 1–3, 2002.

[11] C403/C403M-08, “Standard Test Method for Time of Setting of Concrete Mixtures by Penetration Resistance,” *ASTM Int.*, pp. 1–7, 2008.

[12] ASTM Standard C642, “Standard Test Method for Density, Absorption, and Voids in Hardened Concrete,” *ASTM Int.*, pp. 4–6, 2013.

[13] H. G. Russell, A. R. Anderson, J. O. Banning, J. E. Cook, G. C. Frantz, W. T. Hester, J. Moreno, B. R. Mastin, W. C. Moore, A. H. Nilson, W. F. Perenchio, P. C. Aitcin, F. D. Anderson, R. W. Black, I. G. Cantor, K. D. Drake, T. G. Guennewig, M. D. Luther, C. R. Ohwiler, and M. T. Russell, “State-of-the-Art Report on High-Strength Concrete Reported by ACI Committee 363,” 1997.

[14] J. . Illston and P. L. J. Domone, Eds., *Construction Materials; Their Nature and Behaviour*, Third edit. London: Spon Press, 2001.

[15] D. . Roy, P. Arjunan, and M. . Silsbee, “Effect of silica fume, metakaolin, and low-calcium fly ash on chemical resistance of concrete,” *Cem. Concr. Res.*, vol. 31, no. 12, pp. 1809–1813, Dec. 2001.

[16] T. Nochaiya, W. Wongkeo, and A. Chaipanich, “Utilization of fly ash with silica fume and properties of Portland cement–fly ash–silica fume concrete,” *Fuel*, vol.

89, no. 3, pp. 768–774, Mar. 2010.

[17] a. K. H. Kwan and J. J. Chen, “Adding fly ash microsphere to improve packing density, flowability and strength of cement paste,” *Powder Technol.*, vol. 234, pp. 19–25, Jan. 2013.

[18] S. Mindess, J. F. Young, and D. Darwin, *Concrete*, Second. Prentice Hall, 2003.

[19] F. U. a. Shaikh, S. W. M. Supit, and P. K. Sarker, “A study on the effect of nano silica on compressive strength of high volume fly ash mortars and concretes,” *Mater. Des.*, vol. 60, pp. 433–442, Aug. 2014.

[20] S. H. Lee, H. J. Kim, E. Sakai, and M. Daimon, “Effect of particle size distribution of fly ash–cement system on the fluidity of cement pastes,” *Cem. Concr. Res.*, vol. 33, no. 5, pp. 763–768, May 2003.

[21] H. Toutanji, N. Delatte, S. Aggoun, R. Duval, and a. Danson, “Effect of supplementary cementitious materials on the compressive strength and durability of short-term cured concrete,” *Cem. Concr. Res.*, vol. 34, no. 2, pp. 311–319, Feb. 2004.

[22] F. Sanchez and K. Sobolev, “Nanotechnology in concrete – A review,” *Constr. Build. Mater.*, vol. 24, no. 11, pp. 2060–2071, Nov. 2010.

[23] G. Quercia and H. J. H. Brouwers, “Application of nano-silica (nS) in concrete mixtures,” *8th fib PhD Symp. Kgs. Lyngby, Denmark*, pp. 1–6, 2010.

[24] P. Hou, S. Kawashima, K. Wang, D. J. Corr, J. Qian, and S. P. Shah, “Effects of colloidal nanosilica on rheological and mechanical properties of fly ash–cement mortar,” *Cem. Concr. Compos.*, vol. 35, no. 1, pp. 12–22, Jan. 2013.

[25] A. M. Rashad, “A comprehensive overview about the effect of nano-SiO 2 on some properties of traditional cementitious materials and alkali-activated fly ash,” vol. 52, pp. 437–464, 2014.

[26] ASTM Standard C150/C150M-12, “Standard Specification for Portland Cement,” *ASTM Int.*, p. 9, 2012.

[27] Essroc Italcementi, “Mill Test Report_Type I Cement.pdf,” Dorado, Puerto Rico, 2015.

[28] ASTM Standard C618-12a, “Standard Specification for Coal Fly Ash and Raw or Calcined Natural Pozzolan for Use in Concrete,” *ASTM Int.*, p. 5, 2012.

[29] ASTM Standard C494/C494M-13, “Standard Specification for Chemical Admixtures for Concrete,” p. 10, 2013.

[30] ASTM Standard C33, “Standard Specification for Concrete Aggregates,” *ASTM Int.*, p. 11, 2003.

[31] ASTM Standard C136, “Standard Test Method for Sieve Analysis of Fine and Coarse Aggregates,” *ASTM Int.*, vol. 14, pp. 1–5, 2001.

[32] ASTM Standard C127-15, “Standard Test Method for Relative Density (Specific Gravity) and Absortion of Coarse Aggregate,” *ASTM Int.*, p. 5, 2015.

[33] D. C. Myers, Raymond H. Montgomery, *Response Surface Methodology :process and product optimization using designed experiments*, Second. Wiley-Interscience: John Wiley and Sons, INC., 2002.

[34] ASTM Standard C192, “Standard Practice for Making and Curing Concrete Test Specimens in the Laboratory,” *ASTM Int.*, pp. 1–8, 2005.

[35] D. Montgomery, E. Peck, and G. G. Vining, *Introduction to Linear Regression Analysis*, 5th ed. 2012.

[36] D. Darwin, M. E. Brander, R. W. Carlson, W. L. Clark, and O. R. Werner, “Cracking of Concrete Members in Direct Tension Reported by ACI Committee 224,” vol. 92, no. Reapproved, 1997.

[37] T. . Naik, “Concrete Durability as Influenced by Density and / or Porosity,” *Cem. Concr. Inst. Mex. Symp. "World Concr.*, no. June, p. 13, 1997.

[38] NRMCA, “Time of Setting of Concrete Mixtures,” *Technology in Practice*. [Online]. Available: https://www.nrmca.org/aboutconcrete/downloads/Tip14w.pdf.

[39] M. F. M. Zain, H. B. Mahmud, A. Ilham, and M. Faizal, “Prediction of splitting tensile strength of high-performance concrete,” *Cem. Concr. Res.*, vol. 32, no. 8, pp. 1251–1258, 2002.

[40] M. Ahmed, K. M. El Hadi, M. A. Hasan, J. Mallick, and A. Ahmed, “Evaluating the co-relationship between concrete flexural tensile strength and compressive strength,” *Int. J. Struct. Eng.*, vol. X, pp. 1–17, 2008.

[41] Z. Wu, C. Shi, and W. He, “Comparative study on flexural properties of ultra-high performance concrete with supplementary cementitious materials under different curing regimes,” *Constr. Build. Mater.*, vol. 136, pp. 307–313, 2017.

[42] “How China used more cement in 3 years than the U.S. did in the entire 20th Century - The Washington Post.” [Online]. Available: https://www.washingtonpost.com/news/wonk/wp/2015/03/24/how-china-used-more-cement-in-3-years-than-the-u-s-did-in-the-entire-20th-century/?utm_term=.2abbd49df4f3. [Accessed: 21-Mar-2017].

[43] “High Performance Concrete Market - Global Industry Analysis, Size, Share, Growth, Trends and Forecast 2016 - 2024.” Transparency Market Research, 2016.

[44] P. Zhang, J. Wan, K. Wang, and Q. Li, “Influence of nano-SiO2 on properties of fresh and hardened high performance concrete: A state-of-the-art review,” *Construction and Building Materials*, vol. 148. pp. 648–658, 2017.

[45] H. M. Lim, J. Lee, J.-H. Jeong, S.-G. Oh, and S.-H. Lee, “Comparative Study of Various Preparation Methods of Colloidal Silica,” *Engineering*, vol. 2, no. 12, pp. 998–1005, 2010.

[46] K. Wille, “Development of Non-Proprietary Ultra-High Performance Concrete for Use in the Highway Bridge Sector (FHWA-HRT-13-100),” 2013.

[47] B. Graybeal, “Development of Non-Proprietary Ultra-High Performance Concrete for Use in the Highway Bridge Sector-Tech Brief,” McLean, VA, 2013.

[48] M. M. Yousry and E. Shikh, “Economy of Using High Performance Concrete Economy of Using High Performance Concrete,” 2008.

[49] G. Fischer and V. C. Li, “Influence of matrix ductility on tension-stiffening behavior of steel reinforced engineered cementitious composites (ECC),” *ACI Struct.*, 2002.

[50] P. H. Bischoff, “Tension stiffening and cracking of steel fiber-reinforced concrete,” *ACI Struct.*, pp. 174–182, 2003.

[51] P.-W. Chen and D. D. L. Chung, “Carbon-fiber-reinforced concrete as an intrinsically smart concrete for damage assessment during dynamic loading,” *J. Am. Ceram. Soc.*, no. 78, pp. 816–818, 1995.

[52] W. Yao, J. Li, and K. Wu, “Mechanical properties of hybrid fiber-reinforced concrete at low fiber volume fraction,” *Cem. Concr Res.33*, pp. 27–30, 2003.

[53] M. Tavakkolizadeh and H. Saadatmanesh, “Strengthening of steel-concrete composite girders using carbon fiber reinforced polymers sheets,” *J. Struct. Eng.129*, pp. 30–40, 2003.

[54] L. Lam and J. G. Teng, “Strength models for fiber-reinforced plastic-confined concrete,” *J. Struct. Eng.128*, pp. 612–623, 2002.

[55] N. Plangsriskul and N. Dorsano, “Materials characterization of bamboo and analysis of bonding strength and internal strength as a structural member in reinforced concrete,” 2011.

[56] R. N. Swamy, “Vegetable fibre reinforced cement composites—a false dream or a potential reality?,” in *Vegetable Plants and their Fibres as Building Materials: Proceedings of the Second International RILEM Symposium 7*, 2003, p. 1.

[57] K. Wille and C. Boisvert-Cotulio, “Material efficiency in the design of ultra-high performance concrete,” *Constr. Build. Mater.*, vol. 86, pp. 33–43, 2015.

[58] I. Kaur and R. Siddique, “Mechanical Properties of High Volume Fly Ash (HVFA) Concrete Subjected to Elevated Temperatures up to 120˚C,” M.E. Thesis, Thapar Institute ogf Engineering & Technology University, Patiala, 2005.

[59] A. K. Jassim, “Recycling of Polyethylene Waste to Produce Plastic Cement,” *Procedia Manuf.*, vol. 8, no. October 2016, pp. 635–642, 2017.

[60] EPA, “EPA’s Report on the Environment (2003 Draft),” Washington, DC, 2008.

[61] ASTM Standard C150, “Standard Specification for Portland Cement,” *ASTM Int.*, vol. 86, no. Reapproved 2008, pp. 10–11, 2012.

APPENDICES

A. HIGH STRENGTH BAMBOO FIBER REINFORCED CONCRETE MIXTURES WITH FLY ASH AND SIO_2 NANOPARTICLES PARTIAL REPLACEMENT

A.1 INTRODUCTION

According to the Washington Post, China have used more cement in three years than the US in the entire 20th Century [42]. Cement fabrication accounts for 5 to 10% of the global carbon emission, compelling scientists to devise innovative alternatives with smaller carbon footprints[1]. Therefore, scientists and researchers are studying additions and material replacements to raise the concrete's performance so as to reduce its consumption, thus lowering the overall environmental impact. As it is well known, concrete reinforcement is needed to raise approximately 10% of the material compressive strength. These reinforcements help sustain tensile stresses in a given structural element and prevent or limit crack propagation.

Concrete is usually reinforced with rebar, fibersand mesh from different types of materials such as steel [49], [50] carbon fiber[51]–[53], and polyvinyl chloride [54], among others. Some studies show that steel produces 85 times carbon impact on the environment in the production process than bamboo [55]. Since 1990, bamboo has been considered a potential replacement of steel in concrete [56]. However, as stated by Swamyt, the major concerns in the use of bamboo are related to the lack of adequate bond strength, and its long-term stability [56]. Hence, the present research aimed at increasing such bond strength while minimizing the fiber degradation.

Although researchers have used bamboo as a reinforcing material for concrete, they utilized entire bamboo pieces or bamboo chunks; only a few used bamboo fibers. Of all alternatives, we selected the *Guadua angustifolia* bamboo fiber for this study, since a preliminary research indicated this natural fiber bears better bond strength with minimal fiber degradation. Smaller bamboo elements have a

higher contact area with the concrete matrix that enhances the bond between the two materials. Also, using fiber-reinforced concrete the time and cost of construction can be reduced by the low reinforcement cost. This material can, then, be considered as fiber reinforced concrete (FRC) with fibers aligned in one direction or randomly distributed. The role of randomly distributed discontinuous fibers is to bridge across the cracks that develop upon concrete fracture, regardless of the crack propagation direction. In these conditions, the fibers could lower the crack propagation rate, which increases the deformation of a given concrete element before its final failure[57]. Bridging, as the phenomenon is called, also provides time for replacing the failed part before its total collapse.

This segment of our research focused on understanding the mechanical effect of bamboo fibers (BF) in a high strength concrete matrix.The mechanical characterization of the samples was performed by compressive (ASTM C39) [8] and split tensile tests (ASTM C496) [9].

A.2 METHODOLOGY

A.2.1 Fiber Preparation Process

Guadua angustifolia stems were cut between each node, producing bamboo cylinders of approximately 304 mm in length. Then, these cylinders were sawed through the longitudinal direction to form 76 mm width pieces, as shown in Figure A.1 (A). We soaked these pieces into water for 7 days to make it easier to handle them. After such time, the stem pieces were mechanically rolled to fracture them along the fibers overall direction (stem direction) so as to facilitate the fibers separation. Figure A.1 (B) shows an intermediate stage of a rolled bamboo piece. When some separation between fibers was observed, the distance between the rollers was reduced until the fiber separation was evident, as shown in Figure A.1 (C). The fibers were separated by hand in bundles of around 0.5 - 1 mm, as shown in FigureA.1 (D). Finally, the fibers were cut in approximately 25mm in length for the mixture.

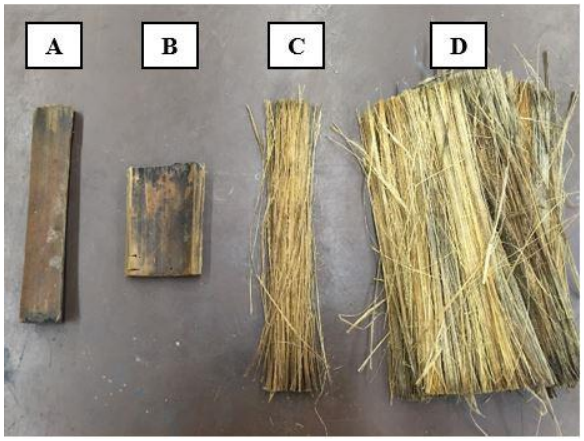

Figure A.1.[A] Bamboo piece, [B] intermediate rolled bamboo piece; [C] final stage of rolled bamboo piece; [D] separated bamboo fibers.

A.2.2 Materials and Mixing Process

The main components of the materials used were Portland cement (PC) type I, fly ash (FA) class F (low-calcium), and nanoparticles of silica (nanostructured SiO_2). As provided, these nanoparticles were opalescent and odorless amorphous silica dispersed in water with an average of 80 nm in diameter. The superplasticizer (SP) was a carboxylate polyether type copolymer, commercially designed as a high-range water-reducing admixture (HRWRA) ADVA 575. Five mixtures with and without fibers containing FA and nS as partial replacement of cement were designed, totaling 10 batches. One percent of bamboo fiber (BF) (by mix weight) was added to the mixes designed to bear those fibers. Table A.1 shows the contents of the five mixture designs from MN1 - MN5; MN refers to Mixture Number.The mixtures weight were sufficient to fill the necessary volume of 18 cylinders of 50mm in diameter and 101mm in height.

To prepare the samples, the coarse and fine aggregates (9.5 mm crush rock and sand combination) were mixed with 2/3 of the required water for 15 seconds at a 120 rpm mixing speed. Then, the cementitious components, i.e. PC, FA, and nS, were added altogether along with the superplasticizer, and mixed for 15 seconds at 60 rpm. Finally, the remaining 1/3 of water and the bamboo fibers were included and mixed for 4.5 minutes at 120 rpm.

Table A.1. Mixture design components

MN	PC (%)	FA (%)	nS (%)
1	54	40	6
2	77	20	3
3	94	0	6
4	60	40	0
5	100	0	0

Then, we poured the mixes into the molds and let them set for 24 hours before demolding. Finally, we placed the specimens into limewater at 25ºC for the curing process for 7, 28, and 90 days prior to the corresponding compressive and split tensile tests.

A.2.3 Compressive and Splitting Tensile Tests

After 7, 28, and 90 curing days we tested the specimens in compression and splittting tensile. Six samples were used for each mechanical test and curing day. In the compressive test, we positioned each sample with its longitudinal axis parallel to the load direction, as shown in Figure A.2 (A). The sample was mounted inside two steel rings and plastic pads to have a better load distribution onto the specimen cross section. For the split tensile test, the specimen was mounted between two wooden plaques (Figure A.2 (B)). As mentioned, the wood pieces applied the linearly distributed load along the sample longitudinal axis.

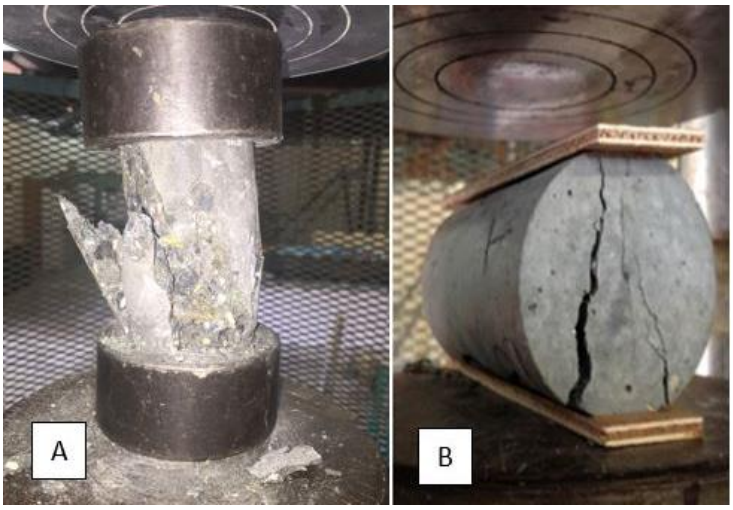

Figure A.2. [A] Compressive test and [B] splitting tensile test

A.3 RESULTS AND DISCUSSION

Optical images of the concrete samples allowed studying the fibers after the mixing procedure. In order to obtain adequate samples that could be used in the microscope, the concrete cylinders were cut with a diamond saw through the longitudinal axis into a disk form. Then, the cut surface was polished to obtain a specular surface for better optical microscopy imaging. Figure A.3 shows that the size of the fibers after the mixing process was 0.1 – 0.5 mm and, upon the molding process, fibers of 1 mm diameter were also observed. This means that the mixing procedure broke the fibers into even smaller pieces. This created a graded size of dispersed fibers in the mixture, which augmented even more the contact area between the hydrated cement and the fibers. The different fiber sizes also multiplied the number of fibers able to bridge between propagating crack surfaces. As it is known, the effectiveness of fiber bridging is when the crack and the fibers bear similar dimensions [18].

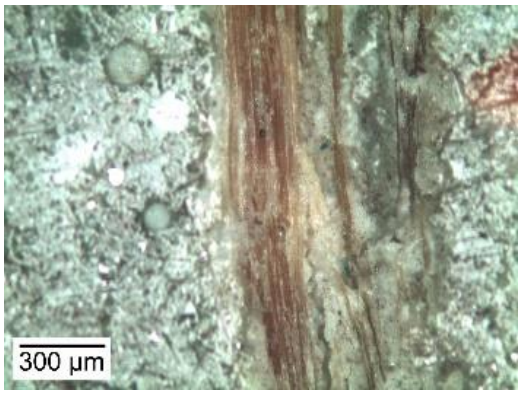

Figure A.3. Optical images of bamboo fibers in concrete

Figure A.4 shows the measured compressive strength of the mixes without and with 1% fiber addition after curing in limewater for 7, 28, and 90 days. As expected, the compressive strength decreased for higher FA levels. In effect, previous research demonstrated that fly ash decreases the amount of cement paste reacting with water to form C-S-H at the early age [58]. However, the inclusion of FA (pozzolan) generates higher amount of C-S-H in concrete and,

hence, longer curing time. This is due to the secondary reaction of the silica present in the fly ash and the calcium hydroxide produced upon cement hydration [18]. Then, nS presence accelerated the pozzolanic reaction leading to a strengthening at the early age [4], [6].

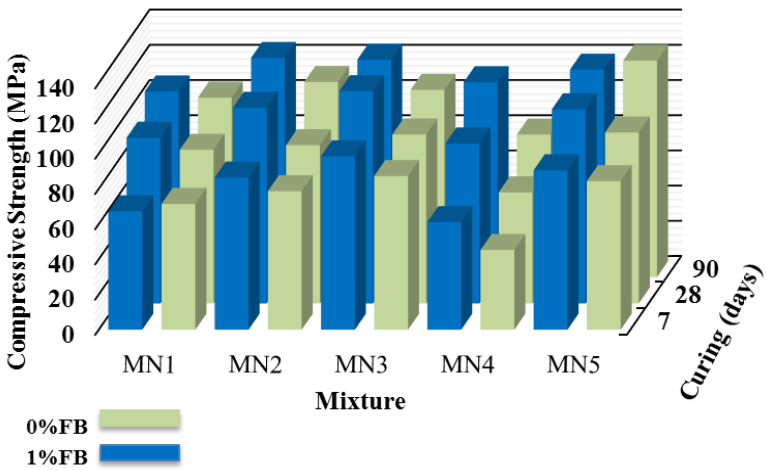

Figure A.4. Compressive strength of mixes without fiber and 1% of fiber addition at 7, 28, and 90 days of curing.

When BF were present, higher compressive strength developed in all mixes. In addition, the fibers favored a faster strength gain, particularly between 7 and 28 days. Both MN-2 and MN-3 have the higher compressive strength at early age when compared to the MN-5 control mix. We attribute this to smaller FA amounts in MN-2 and the presence of nS in both MN-2 and MN-3.

Table A.2 shows the average percent strength gain in mixes with and without fibers at 28 days. The MN-4 mix (40% FA) showed lower compressive strength than MN-5, which was expected. One deems important to note that when BF are added to the concrete even the weakest mix, i.e. MN-4, presented a noteworthy increase in mechanical strength at all curing ages. The compressive strength displayed a 44% increment at 28 days (Table A.2). The MN-5 mix with BF showed a 14% compressive strength gain at 28 days, accompanied with a slight decrease at 90 days.

MN-1 with 40% FA (the highest FA level as replacement), 6% nS, and BF developed around 50 % more strength when compared to MN4 that had no fiber.

Such difference in strength between these two mixes demonstrated that nanostructured silica did acelerate the reaction and produced a higher concentration of C-S-H in concrete. The addition of small nS amount caused a significant effect in the overall strength of concrete at short and long term. Nevertheless, even with this overall strength increase, the BF addition only helped raise the compression strength by 8% at 28 days (mixture MN-1).

Table A.2. Average percent strength increment of mixes with fiber compared to the mixes without BF at 28 days of curing

Strength	**MN1**	**MN2**	**MN3**	**MN4**	**MN5**
Compressive	8%	24%	26%	44%	14%
Splitting Tensile	19%	9%	16%	28%	13%

Further, we measured the splitting tensile strength at 7, 28, and 90 days of curing in limewater (Figure A.5). Our results shows that 1% BF addition lowered the tensile strength at the early age in MN-1, MN-2 and MN-3 mixes. Conversely, MN-4 and MN-5 presented a slight tensile strength gain at early age. The split tensile strength is around the expected values of 10% of the compressive strength according to the ACI 318. The MN-3 with 1% BF reached a 16% tensile strength gain at 28 days and 37% at 90 days when compared with the mix without fiber. The maximum values of tensile strength at 28 and 90 days were found on the mixtures bearing nS and BF.

Such boost in both compressive and tensile strengths shows that the randomly distributed BF are working as an effective reinforcement for concrete. The fibers were effective crack bridges within the concrete matrix, hindering crack propagation, and leading to higher mechanical strength. In general, the addition of bamboo fibers to high strength concrete with high fly ash contents raised their strength remarkably. Moreover, the BF presence in mixtures containing high FA contents can be further improved with partial PC replacement with silica nanoparticles.

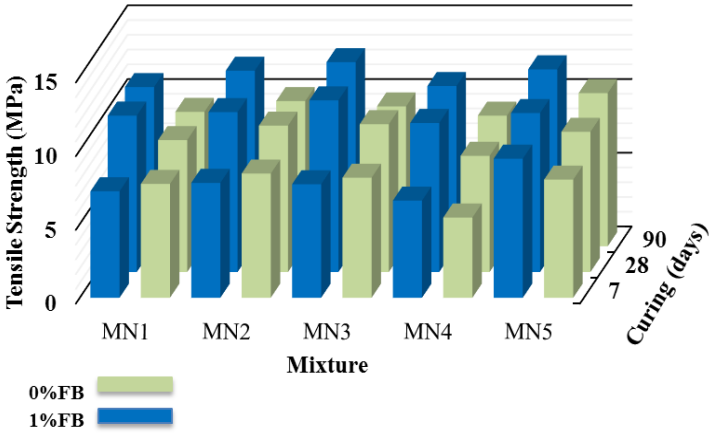

Figure A.5. Splitting tensile strength results of mixes without fiber and 1% of fiber addition at 7, 28, and 90 days of curing.

A.4 CONCLUSIONS

It has been proved that the addition of the bamboo fibers to concrete produced higher compressive and split tensile strengths in the mixtures. The data shows a 22% increment in average compressive strength and a mean 17% improvement of tensile strength. This enhancement is attributed to the fibers bridging, which hampers the crack propagation in the hardened cement matrix. These beneficial effect of the bamboo fibers is more manifest in mixtures with lower mechanical properties.

The difference in mechanical strength among all mixtures is chiefly a result of the constituent materials present in each mixture. For instance, the presence of nanostructured silica increases the mechanical properties of the mixture, which is apparent in the difference between the compressive strengths of MN-1 (40%FA,6%nS) and MN-4 (40%FA, 0%nS).

The procedure used to obtain the fiber has a potential to be industrialized and accelerate the fabrication of the bamboo fiber-containing concrete. In summary, the addition of bamboo fibers is a low cost solution to increase the fracture resistance of a concrete mixture.

B. DESIGN AND CHARACTERIZATION OF CONCRETE MASONRY PARTS USING PLASTIC AS AGGREGATE

B.1. INTRODUCTION

The overuse of plastic products has caused large waste accumulation, which are of increasing environmental concern. Plastic material is categorized in many types that can be recyclable, reusable, and disposable. The disposable only type of plastic is known to have a long degradation time. Accumulation of this type of plastics raises challenges and opportunities that that will be addressed in this document. Recycling companies indicated that the only option for those types of plastics that cannot be reused is to shred them and discarding them back to the landfill.

Plastics are materials with appealing properties: low density, durability, low cost of production, workability, and ability to be molded in different forms in viscous state. This made the material ideal for applications in the automotive, aeronautical, food, and pharmaceutical industries. However, this material generates post-consumer waste that is producing a worldwide environmental pollution problem, mainly because most plastics do not degrade easily [59]. Recycling is an alternative to prevent the disposal end of these plastics either in landfills or water bodies that are finally connected with the oceans. According to some studies, global consumption of plastics increased from 5 million tons in the 1950s to almost 100 million tons in 2001[59]. EPA in 2003 revealed that in the United States 80% of plastic used is discarded in landfills, 8% is incinerated, and only 7% is recycled [60].

Furthermore, concrete is one of the building materials of greatest demand in the world. Its manufacturing process causes approximately 5-10% of CO_2 emitted into the atmosphere [1]. In unstable economies, the constant infrastructure development can represent a big challenge when trying to keep track of project expenditures. Because of this, many materials scientists and engineers are constantly seeking to optimize construction time and reduce materials consumption. The environmental issues that arise every day, and that have to be accounted for on every project, also represent a major factor to be considered.

Accordingly, many engineers have sought to reduce the negative effects of concrete production by incorporating recycled materials such as: plastics, crushed rubber, and coal incineration products (from energy production), among others. As a response to the amount of contamination and the lack of innovation for the development of infrastructure, an opportunity for possible solution to this problem comes forth.

In this project, the University of Puerto Rico at Mayagüez (UPRM) collaborates with Reciclaje del Norte (RDN) Company in order to develop a new product. This is a composite that incorporates different categories of recyclable plastic such as PET carbon, pallets and a plastic mixture combined with sand, cement and/or aggregate (gravel). Although plastics are not commonly used in structures or as an aggregate in structural elements, we sought to develop an eco-brick, mixture, block, or non-structural piece. If the product proves to be effective, it will be an alternative to mitigate plastic accumulation in the environment.

B.2. ECO-BRICKS

B.2.1. METHODOLOGY

Materials

The main plastic studied in this research is the one supplied for RDN Company, particularly the ones with the denominations of PET carbon, pallets, and mixture. Other parts of the mix are Portland cement (PC) type I (ASTM C150[61]) and sand bearing a fineness modulus of 1.95 as fine aggregate (ASTM C136 [31]). Table B.1 shows the densities of the materials used in this project and Table B.2 depicts preliminary mixture design for the bricks.

Table B.1. Materials Density

Code	Description	Density (gr/cm^3)
PC	Portland Cement	3.180
S	Sand	1.580
PL#1	HDPE	0.315
PL#2	PET Carbon	0.345
PL#3	Pallets #7	0.476
PL#4	Mix	0.324

PL#5	Other Plastics	0.406

Table B.2. Mixture design for eco-bricks (proportions by weight)

CODE	Portland Cement	Sand	Plastic	Water
PL#2-C1	1	2	0.250	9-10%
PL#2-C2	1	2	0.125	9-10%
PL#2-C3	1	1.5	0.250	9-10%
PL#2-C4	1	1	0.250	9-10%
PL#3-C1	1	2	0.250	9-10%
PL#3-C2	1	2	0.300	9-10%
PL#4-C1	1	2	0.250	9-10%
PL#4-C2	1	2	0.125	9-10%

Mixing Procedure

For the concrete mix preparation we used a 5L Globe sp-20 mixer machine operated at 60 and 120 rpm cycling speeds. The mixture started by adding the aggregates and the Portland cement (PC) and thereupon mixing it at 60 rpm for fifteen seconds. Afterwards, we added water to the mixture while mixing continued at 120 rpm for 3 minutes until the mix appeared wet. This was placed in the receiving tank of an ECO Brava brick machine in a sealed chamber where hydraulic pressure was applied to reduce pore space, densify the mix, and consolidate the brick. The final brick dimensions were 76 mm height, 101 mm width, and 203 mm length.

Once the bricks were ready we inspected them visually. The bricks must slide off the mold without cracking or breaking. After every type of mixture the brick machine was cleaned out to prevent any malfunction of the moving mechanisms.

Mechanical Characterization

The bricks resistance was evaluated via a compression test, as the compressive strength is the most important property for the characterization of bricks. This test was done in a 3000 kN Forney universal test machine using ASTM C140 standards. The test uses one metallic plate over the brick sample which distributes the applied load evenly. The compression strength was then

calculated using the maximum measured load before fracture divided by the cross sectional area of brick. This compression test was performed in the samples (brick) at 3 and 7 days of curing ages.

B.3.2 RESULTS AND DISCUSSIONS

During the early stages of the project we sketched prospective levels of sand, plastic and water in mixes by weight of cement to be used in the bricks. The manufacturing of these mixtures allowed us to observe the lack of cohesion of the plastic with the matrix (sand / cement). These mixtures resulted in a brittle brick that could not be handled. The ratio used as a reference for these preliminary tests was 1:3 of cement and sand, which is commonly used in conventional bricks. Therefore, for the next step we changed those levels to one that would allow better consolidation of the materials mixture in the machine and that will eventually produce a better element (brick). In that first instance, we used a1:2 (cement / sand) mixture with 50% plastic. This percentage caused a lack of cohesion between the materials, causing the bricks to crack and break before being removed from the mold. Subsequently, the previous proportion of sand and cement was used with only 25% plastic. The block manufacturing was not sufficient for a good quality brick with the exception of the mixture PL # 3-C1 (pallets), which had a good compaction and the brick could be removed from the mold. Finally, the amount of plastic was reduced to 12.5% for the mixes containing PET Carbon and mixed plastics. Figure B.1 shows the volume percent of each material in the eco-bricks studied.

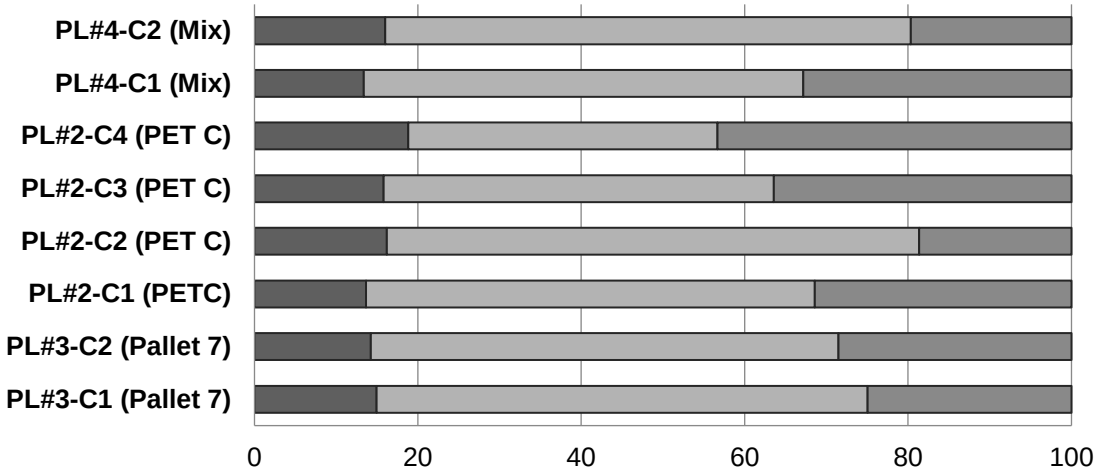

	PL#3-C1 (Pallet 7)	PL#3-C2 (Pallet 7)	PL#2-C1 (PETC)	PL#2-C2 (PET C)	PL#2-C3 (PET C)	PL#2-C4 (PET C)	PL#4-C1 (Mix)	PL#4-C2 (Mix)
PC (%)	15	14	14	16	16	19	13	16
Sand (%)	60	57	55	65	48	38	54	64
PL (%)	25	29	31	19	36	43	33	20

Figure B.1. Volume percent of Portland cement, sand and type of plastic in the eco-bricks first designs.

In this case, the brick were properly produced and were tested under compression for 3 and 7 days of curing time. Table B.3 describes the observations found in the samples during the bricks manufacturing and Figure B.2 presents the initial results of the specimens, which generally exceeded 13.8 MPa (2,000 psi) of compressive strength. In the bricks with PET Carbon plastic (PL#2), the smooth and laminar shape of the material pieces was detrimental to the cohesion with the matrix. Therefore, this brick should have a plastic percentage not higher than 19-20% by volume of the brick. In the bricks containing mixed plastics (PL#4), the cohesiveness between the plastic and the matrix was also affected. The main challenge in this case was to make the brick avoiding cracks due to expansion. This expansion resulting from elastic recovery of the rubber-type pieces. While making the brick it was very difficult to remove it from the mold without breaking it. The plastic percent should not exceed 20% of the volume of the brick to make it manageable. Finally, in the bricks with Pallets 7 (PL#3), one noticed that the particular shape and size of the plastic pieces, very similar to gravel, favored its addition to the brick mixtures, making this one the best recycling options for the bricks. These bricks were very easy to handle and

from the beginning showed very good cohesiveness. This brick can hold up to 30% by volume of plastic.

Table B. 3. Proportions by weight, percent of plastic and observations summary during brick fabrication

CODE	Proportion PC:Sand:Plastic	Plastic (%Volume)	Water	Observations
PL#2-C1	1 : 2 : 0.250	31	9-10%	Regular compaction (is fragile) Poor mobility (cracking)
PL#2-C2	**1 : 2 : 0.125**	**19**	**9-10%**	**Good compaction (seems solid)**
PL#2-C3	1 : 2 : 0.250	36	9-10%	Regular compaction (is fragile) Poor mobility (cracking)
PL#2-C4	1 : 2 : 0.250	43	9-10%	Regular compaction (is fragile) Better mobility (cracking)
PL#3-C1	1 : 2 : 0.250	25	9-10%	Excellent compaction Excellent mobility
PL#3-C2	**1 : 2 : 0.300**	**29**	**9-10%**	**Excellent compaction Excellent mobility**
PL#4-C1	1 : 2 : 0.250	33	9-10%	Poor compaction (not working)
PL#4-C2	**1 : 2 : 0.125**	**20**	**9-10%**	**Regular compaction (is fragile)**

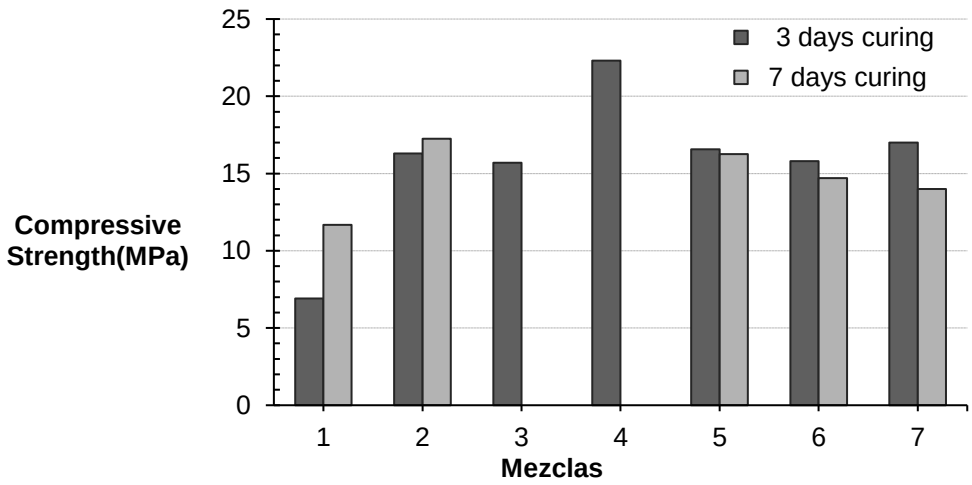

Figure B.2. Compressive strength of bricks according to the plastic type used

B.2.3 COST ESTIMATE

Some costs were evaluated to validate the possibility of marketing the product. Only material costs were included. The cost estimate shows in the Table 4 was based with the following unit values of the materials:

Sand: 0.04 $/kg

Portland cement: 0.17 $/kg

Plastic: 0.14$/kg

Table B.4. Proportions by volume and summary of cost for the eco-brick

	Proportions (Volumen)			Cost $			
Mixture	PC (%)	Sand (%)	PL (%)	PC	Sand	PL	**Total**
PL#3-C1 (Pallet 7)	15	60	25	0.13	0.06	0.03	0.21
PL#3-C2 (Pallet 7)	**14**	**57**	**29**	**0.12**	**0.06**	**0.03**	**0.21**
PL#2-C1 (PETCarbon)	14	55	31	0.12	0.05	0.02	0.19
PL#2-C2 (PET Carbon)	**16**	**65**	**19**	**0.14**	**0.06**	**0.01**	**0.22**
PL#2-C3 (PETCarbon)	16	48	36	0.13	0.05	0.03	0.21
PL#2-C4 (PETCarbon)	19	38	43	0.16	0.04	0.03	0.23
PL#4-C1 (Mix)	13	54	33	0.11	0.05	0.02	0.19
PL#4-C2 (Mix)	**16**	**64**	**20**	**0.14**	**0.06**	**0.01**	**0.21**

B.3. CONCRETE MIX

B.3.1. METHODOLOGY

Materials and Mixing Process

The main plastic studied, particularly the ones with mixture plastics, were supplied by RDN Company. The main components of the materials used were Portland cement (PC) type I, fly ash (FA) class F (low-calcium), nanoparticles of silica (nanostructured SiO_2) and coarse and fine aggregates (9.5 mm crush rock and sand combination). As provided, these nanoparticles were opalescent and odorless amorphous silica dispersed in water. Table B.5 shows the contents of the six mixture designs from MN1 – MN6; MN refers to Mixture Number. As observed, 50 and 100 percent of coarse aggregate were replaced in the different mixtures.

To prepare the samples, the coarse and fine aggregates and plastic were mixed with 2/3 of the required water for 15 seconds at a 120 rpm mixing speed. Then, the cementitious components, i.e. PC, FA, and nS, were added altogether along with the superplasticizer, and mixed for 15 seconds at 60 rpm. Finally, the remaining 1/3 of water were added and mixed for 4.5 minutes at 120 rpm.

Table B.5. Contents of mixtures designs

Mix Number	% Plastic	% Gravel	PC	FA	nS
MN1	50	50	50	50	0
MN2	50	50	47	50	3
MN3	50	50	100	0	0
MN4	100	0	50	50	0
MN5	100	0	47	50	3
MN6	100	0	100	0	0

Thereupon, we poured the mixes into the molds and let them set for 24 hours before demolding. Finally, we placed the specimens into limewater for the curing process for 3, 7, and 14 days prior to the corresponding compressive and split tensile tests.

B.4. COMPRESSIVE AND TENSILE STRENGTH OF CONCRETE WITH PLASTIC AS AGGREGATE REPLACEMENT

After realizing that some of the plastics studied were not very favorable to be considered within the bricks, we decided to start assessing a fluid mixture and tried to acquire structural strength (23 MPa). In these mixtures the coarse aggregate was substituted with plastic and its behavior was evaluated with compression and tension tests. Figures B3 and B4 show the compression and tension results. An average of 50% decrease in compression resistance is noticeable when replacing 100% of the coarse aggregate by plastic. However, the results show that when using only 50% replacement, very favorable results were obtained, which were nigh to the structural resistance goal. These auspicious results can be better seen in the mixture MN3 that contains 100% cement, which is to be expected since the others with fly ash lowered its

resistance gain. The nanoparticles (in specimens MN2) appear to have no strong influence on the resistance gain within these mixtures.

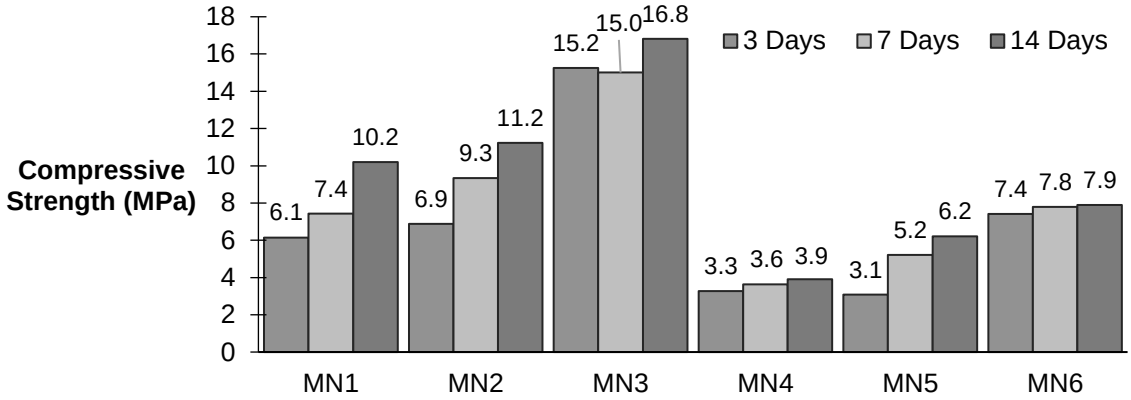

Figure B.3. Compressive strength for mixes with 50% and 100% of coarse aggregate replacement by plastic at 3, 7 and 14 days.

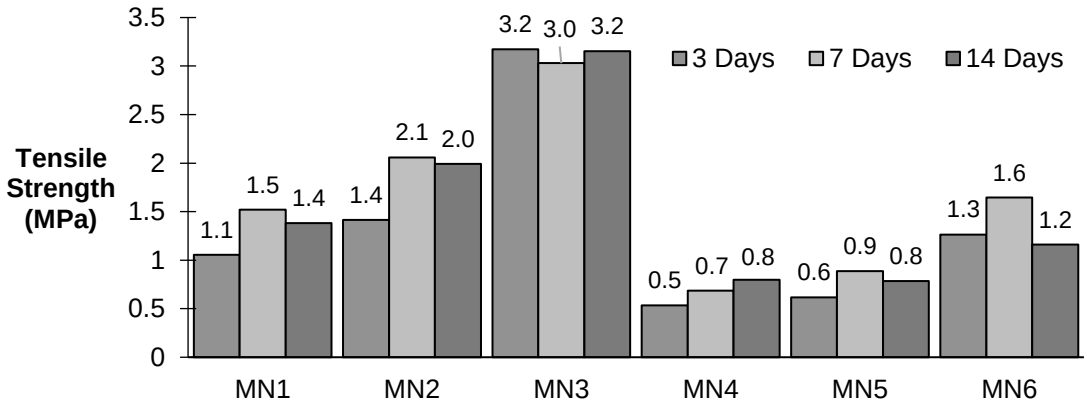

Figure B.4. Splitting tensile strength for mixes with 50% and 100% of coarse aggregate replacement by plastic at 3, 7, and 14 days.

B.5. CONCLUSIONS

- The results showed that in order to obtain a brick bearing the required strength according to the specifications, different amounts of plastic are required in the mixtures depending on the type of plastic.

- In this study a weight ratio of 1:2:0.125 (PC:Sand:PL) is ideal when producing a brick with **PET Carbon** plastic.

- In the bricks containing **mixed plastics**, a weight ratio of 1:2:0.125 (PC: Sand: PL) was necessary for optimum results when fabricating the brick.

- Finally, in the bricks with **pallets 7**, resulted in a ratio by weight of 1:2:0.30 (PC: Sand: PL) when fabricating a brick with this plastic.

- The results obtained in the compression tests exceeded the strength of 23.8 MPa (2,000 psi), minimum value for the structural concrete solid bricks [ASTM C55 14a].

- When we consider a fluid mixture with possibilities of achieving structural strength, we can conclude that it is better to consider not replacing 100% of the coarse aggregate with plastic due to its loss of more than 50% strength. Given the results of this research, we can consider an optimization of mixtures where we can achieve structural strength with the optimum amount of materials.